
VIMA: GENERAL ROBOT MANIPULATION WITH MULTIMODAL PROMPTS

Yunfan Jiang^{1,2*}, Agrim Gupta^{2†}, Zichen Zhang^{3†}, Guanzhi Wang^{1,4†}, Yongqiang Dou⁵,

Yanjun Chen², Li Fei-Fei², Anima Anandkumar^{1,4}, Yuke Zhu^{1,6‡}, Linxi Fan^{1‡}

¹NVIDIA, ²Stanford, ³Macalester College, ⁴Caltech, ⁵Tsinghua, ⁶UT Austin

† Equal contribution ‡ Equal advising

<https://vimalabs.github.io>

ABSTRACT

Prompt-based learning has emerged as a successful paradigm in natural language processing, where a single general-purpose language model can be instructed to perform any task specified by input prompts. Yet task specification in robotics comes in various forms, such as imitating one-shot demonstrations, following language instructions, and reaching visual goals. They are often considered different tasks and tackled by specialized models. This work shows that we can express a wide spectrum of robot manipulation tasks with *multimodal prompts*, interleaving textual and visual tokens. We design a transformer-based generalist robot agent, VIMA, that processes these prompts and outputs motor actions autoregressively. To train and evaluate VIMA, we develop a new simulation benchmark with thousands of procedurally-generated tabletop tasks with multimodal prompts, 600K+ expert trajectories for imitation learning, and four levels of evaluation protocol for systematic generalization. VIMA achieves strong scalability in both model capacity and data size. It outperforms prior SOTA methods in the hardest zero-shot generalization setting by up to $2.9\times$ task success rate given the same training data. With $10\times$ less training data, VIMA still performs $2.7\times$ better than the top competing approach. We open-source all code, pretrained models, dataset, and simulation benchmark at <https://vimalabs.github.io>.

1 INTRODUCTION

Transformers have given rise to remarkable multi-task consolidation across many AI domains. For example, users can describe a task using natural language prompt to GPT-3 (Brown et al., 2020), allowing the same model to perform question answering, machine translation, text summarization, etc. Prompt-based learning provides an accessible and flexible interface to communicate a natural language understanding task to a general-purpose model.

We envision that a generalist robot agent should have a similarly intuitive and expressive interface for task specification. What does such an interface for robot learning look like? As a motivating example, consider a personal robot tasked with household activities. We can ask the robot to bring us a cup of water by a simple natural language instruction. If we require more specificity, we can instead instruct the robot to “bring me <image of the cup>”. For tasks requiring new skills, the robot should be able to adapt preferably from a few video demonstrations (Duan et al., 2017). Tasks that need interaction with unfamiliar objects can be easily explained via a few image examples for *novel concept grounding* (Hermann et al., 2017). Finally, to ensure safe deployment, we can further specify visual constraints like “do not enter <image> room”.

To enable a single agent with all these capabilities, we make three key contributions in this work: 1) a novel **multimodal prompting formulation** that converts a wide spectrum of robot manipulation tasks into one sequence modeling problem; 2) a new **robot agent model** capable of multi-tasking and zero-shot generalization; and 3) a **large-scale benchmark** with diverse tasks to systematically evaluate the scalability and generalization of our agents.

*Work done during NVIDIA internship.

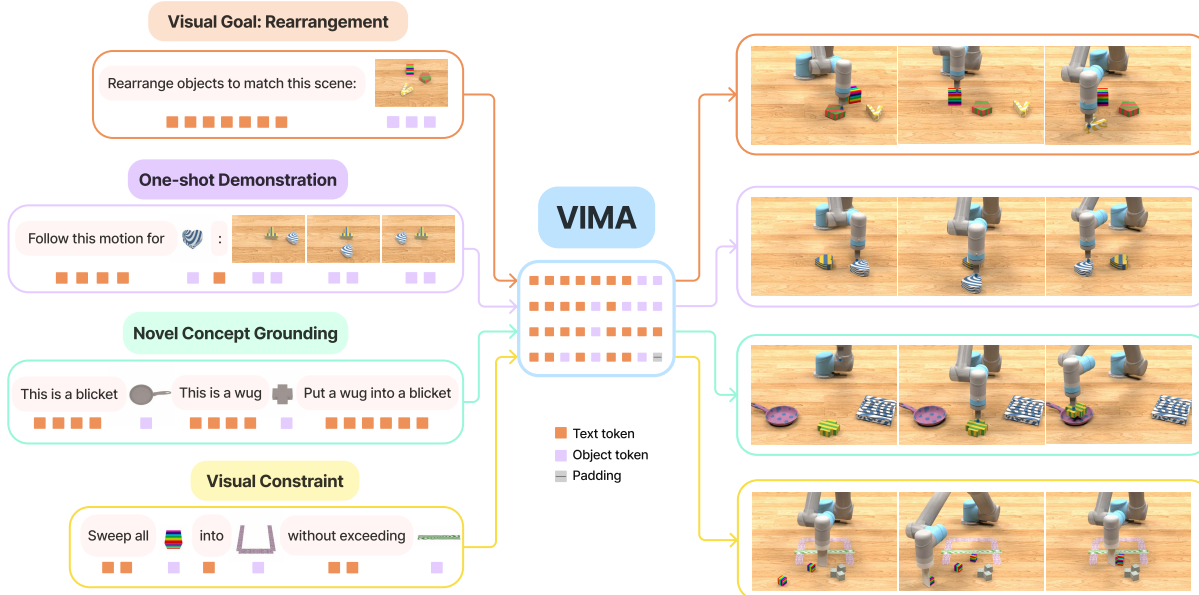


Figure 1: **Multimodal prompts for task specification.** We observe that many robot manipulation tasks can be expressed as *multimodal prompts* that interleave language and image/video frames. We propose VIMA, an embodied agent model capable of processing multimodal prompts (left) and controlling a robot arm to solve the task (right).

We start with the observation that many robot manipulation tasks can be formulated by **multimodal prompts that interleave language and images or video frames** (denoted by “{image}” in Fig. 1). For example, Rearrangement (Batra et al., 2020), a type of *Visual Goal*, can be formulated as “Please rearrange objects to match this {scene.image}”; *Novel Concept Grounding* looks like “This is a dax {new_object}₁ and this is a blicket {new_object}₂. Put two metal dax on the marble blicket.”; *Few-shot Imitation* can embed video snippet in the prompt “Follow this motion trajectory for the wooden cube: {frame₁}, {frame₂}, {frame₃}, {frame₄}”; and expressing *Visual Constraint* is as simple as adding the clause “without touching {safety_boundary}”.

Multimodal prompts not only have more expressive power than individual modalities, but also enable a **uniform sequence IO interface** for training generalist robot agents. Previously, different robot manipulation tasks require distinct policy architectures, objective functions, data pipelines, and training procedures (Aceituno et al., 2021; Stengel-Eskin et al., 2022; Lynch & Sermanet, 2021), leading to siloed robot systems that cannot be easily combined for a rich set of use cases. Instead, our multimodal prompt interface allows us to harness the latest advances in large transformer models (Lin et al., 2021; Tay et al., 2020; Khan et al., 2021) for developing scalable multi-task robot learners.

To this end, we design a novel **VisuoMotor Attention model** (VIMA, reads “v-eye-ma”). The architecture follows the encoder-decoder transformer design proven to be effective and scalable in NLP (Raffel et al., 2020). VIMA encodes an input sequence of interleaving textual and visual prompt tokens with a pretrained language model (Tsimploukelli et al., 2021), and decodes robot control actions autoregressively for each environment interaction step. The transformer decoder is conditioned on the prompt via cross-attention layers that alternate with the usual causal self-attention. Instead of operating on raw pixels, VIMA adopts an object-centric approach. We parse all images in the prompt or observation into objects by off-the-shelf detectors (He et al., 2017), and flatten them into sequences of object tokens. All these design choices combined deliver a conceptually simple architecture with strong model and data scaling properties.

To systematically evaluate our proposed algorithm, we introduce a new benchmark (VIMA-BENCH) built on the Ravens simulator (Zeng et al., 2020; Shridhar et al., 2021). We provide 17 representative meta-tasks with multimodal prompt templates, which can be procedurally instantiated into thou-

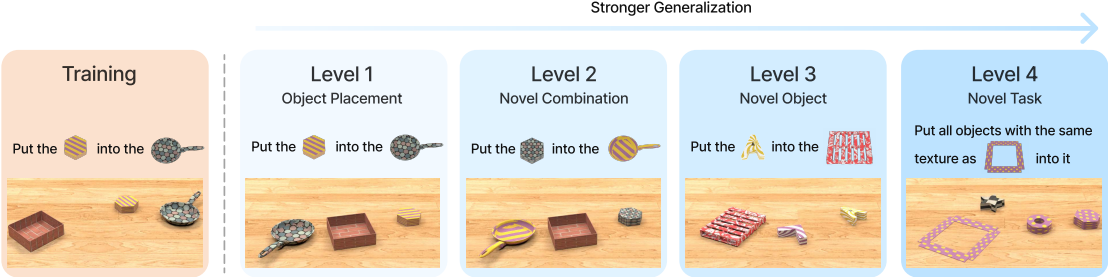


Figure 2: **Evaluation Protocol in VIMA-BENCH.** We design 4 levels of evaluation settings to measure the zero-shot generalization capability of an agent systematically. Each level deviates more from the training distribution, and thus is strictly more challenging than the previous level.

sands of individual tasks by various combinations of textures and tabletop objects. VIMA-BENCH establishes a 4-level protocol to evaluate progressively stronger generalization capabilities, from randomized object placement to novel tasks altogether (Fig. 2). To demonstrate the scalability of VIMA, we train a spectrum of 7 models ranging from 2M to 200M parameters. Our approach outperforms strong prior SOTA methods such as Gato (Reed et al., 2022), Decision Transformer (Chen et al., 2021), and Flamingo (Alayrac et al., 2022) across all 4 levels of zero-shot generalization and all model capacities, sometimes by a large margin (up to $2.9\times$ task success rate given the same amount of training data, and $2.7\times$ better even with $10\times$ less data). We open-source the simulation suite, training dataset, algorithm implementation, and pretrained model checkpoints to ensure reproducibility and facilitate future works from the community.

2 MULTIMODAL PROMPTS FOR TASK SPECIFICATION

A central and open problem in robot learning is task specification (Agrawal, 2022). Our key insight is that various task specification paradigms (such as goal conditioning, video demonstration, natural language instruction) can all be instantiated as multimodal prompts (Fig. 1). Concretely, a multimodal prompt \mathcal{P} of length l is defined as an ordered sequence of arbitrarily interleaved texts and images $\mathcal{P} := [x_0, x_1, \dots, x_l]$, where each element $x_i \in \{\text{text}, \text{image}\}$.

Task Suite. The flexibility afforded by multimodal prompts allows us to specify and build models for a huge variety of task specification formats. Here we consider the following six task categories:

1. **Simple object manipulation:** simple tasks like “put <object> into <container>”, where each image in the prompt corresponds to a single object;
2. **Visual goal reaching:** manipulating objects to reach a goal configuration, e.g., *Rearrangement* (Batra et al., 2020);
3. **Novel concept grounding:** the prompt contains unfamiliar words like “dax” and “bicket”, which are explained by in-prompt images and then immediately used in an instruction. This tests the agent’s ability to rapidly internalize new concepts;
4. **One-shot video imitation:** watching a video demonstration and learning to reproduce the same motion trajectory for a particular object;
5. **Visual constraint satisfaction:** the robot must manipulate the objects carefully and avoid violating the (safety) constraints;
6. **Visual reasoning:** tasks that require reasoning skills, such as appearance matching “move all objects with same textures as <object> into a container”, and visual memory, “put <object> in container and then restore to their original position”.

Note that these six categories are not mutually exclusive. For example, a task may introduce a previously unseen verb (*Novel Concept*) by showing a video demonstration, or combine goal reaching with visual reasoning. More details about the task suite are discussed in Appendix, Sec. B.

3 VIMA-BENCH: BENCHMARK FOR MULTIMODAL ROBOT LEARNING

Simulation Environment. Existing benchmarks are generally geared towards a particular task specification. To our knowledge, there is no benchmark that provides a rich suite of multimodal tasks and a comprehensive testbed for targeted probing of agent capabilities. To this end, we introduce a new benchmark suite for multimodal robot learning that we call VIMA-BENCH. We built our benchmark by extending the Ravens robot simulator (Zeng et al., 2020; Shridhar et al., 2021). VIMA-BENCH supports extensible collections of objects and textures to compose multimodal prompts and procedurally generate a large number of tasks. Specifically, we provide 17 meta-tasks with multimodal prompt templates, which can be instantiated into 1000s of individual tasks. Each meta-task belongs to one or more of 6 task specification methods mentioned above. VIMA-BENCH can generate large quantities of imitation learning data via scripted oracle agents. More details are elaborated in Appendix, Sec. A.

Observation and Actions. The observation space of our simulator includes RGB images rendered from both frontal view and top-down view. Groundtruth object segmentations and bounding boxes are also provided for training object-centric models (Sec. 4). We inherit the high-level action space from Zeng et al. (2020), which consists of primitive motor skills like “pick and place” and “wipe”. These are parameterized by poses of the end effector. Our simulator also features scripted oracle programs that can generate expert demonstrations by using privileged simulator state information, such as the precise location of all objects, and the groundtruth interpretation of the multimodal instruction.

Training Dataset. We leverage the pre-programmed oracles to generate a large offline dataset of expert trajectories for imitation learning. Our dataset includes 50K trajectories per meta-task, and 650K successful trajectories in total. We hold out a subset of object models and textures for evaluation, and designate 4 out of 17 meta-tasks as a testbed for zero-shot generalization.

Evaluating Zero-Shot Generalization. Each task in VIMA-BENCH has a binary success criterion and does not provide partial reward signals. During test time, we execute the agent policies in the physics simulator for multiple episodes to compute a success rate in percentage. The average success rate over all evaluated meta-tasks will be the final reported metric.

We design a 4-level evaluation protocol (Fig. 2) to systematically probe the generalization capabilities of learned agents. Each level deviates more from the training distribution, and is thus strictly harder than the previous one:

1. **Placement generalization:** all prompts are seen verbatim during training, but only the placement of objects on the tabletop is randomized at testing.
2. **Combinatorial generalization:** all materials (adjectives) and 3D objects (nouns) are seen during training, but new combinations of them appear in testing.
3. **Novel object generalization:** test prompts and the simulated workspace include novel adjectives and objects.
4. **Novel task generalization:** new meta-tasks with novel prompt templates at test time.

4 VIMA: VISUOMOTOR ATTENTION MODEL

Our goal is to build a robot agent which can perform any task specified by multimodal prompts. To learn an effective multi-task robot policy, we propose VIMA, a minimalistic multi-task encoder-decoder architecture with object-centric design (Fig. 3). Concretely, we learn a robot policy $\pi(a_t|\mathcal{P}, \mathcal{H})$, where $\mathcal{H} := [o_1, a_1, o_2, a_2, \dots, o_t]$ denotes the past interaction history, and $o_t \in \mathcal{O}$, $a_t \in \mathcal{A}$ are observations and actions at each interaction steps. We encode the prompt via a frozen pre-trained language model and decode the robot motor commands conditioned on the encoded prompt via cross-attention layers.

Tokenization. There are 3 formats of raw input in the prompt — text, image of a single object, and image of a full tabletop scene (e.g., for *Rearrangement* or imitation from video frames). For **text inputs**, we use pre-trained T5 tokenizer and word embedding to obtain word tokens. For **images of full scenes**, we first extract individual objects using off-the-shelf Mask R-CNN (He et al., 2017). Each object is represented as a bounding box and a cropped image. We then compute object tokens

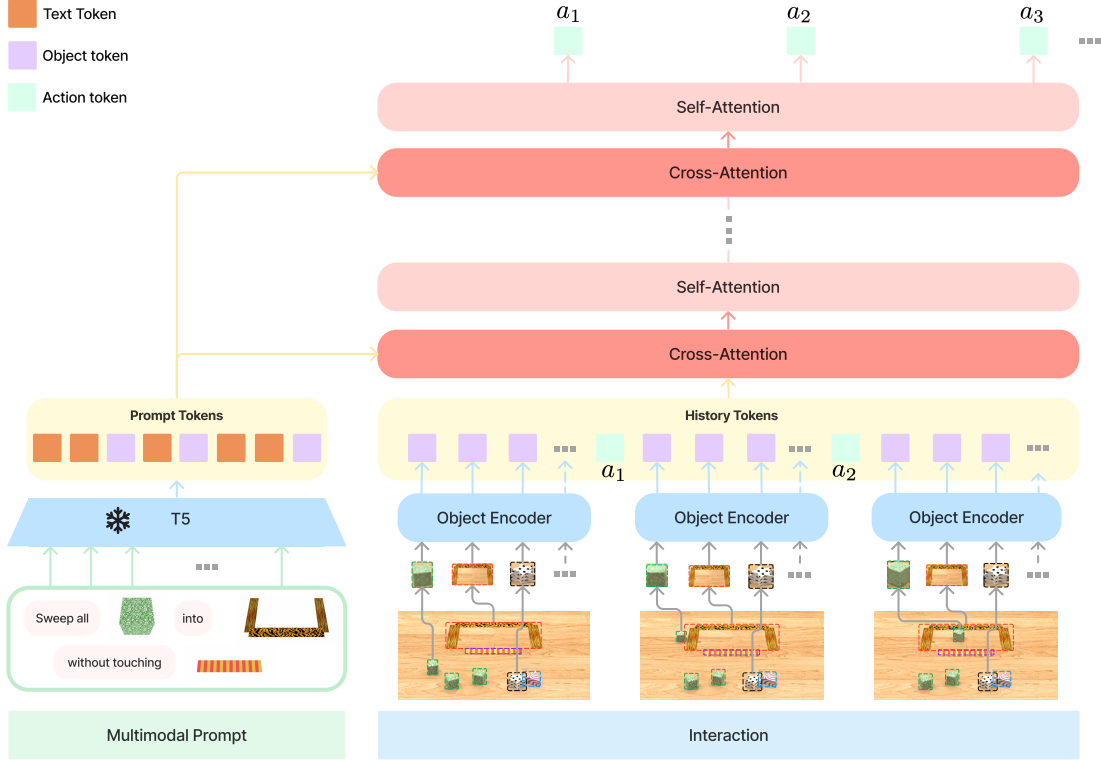


Figure 3: **VIMA**. We encode the multimodal prompts with a pre-trained T5 model, and condition the robot controller on the prompt through cross-attention layers. The controller is a causal transformer decoder consisting of alternating self and cross attention layers that predicts motor commands conditioned on prompts and interaction history.

by encoding them with a bounding box encoder and a ViT, respectively. For **images of single objects**, we obtain tokens in the same way except with a dummy bounding box. We then follow [Tsimpoukelli et al. \(2021\)](#) to produce prompt encoding by passing the resulted token sequence to a pre-trained T5 encoder model. Our positional embedding is learnable and absolute.

Robot Controller. A challenging aspect of designing multi-modal multi-task policy is to select a suitable conditioning mechanism. In our schema (Fig. 3), the robot controller (decoder) is conditioned on the prompt sequence \mathcal{P} by a series of cross-attention layers between \mathcal{P} and the trajectory history sequence \mathcal{H} . Each cross-attention layer generates an output sequence $\mathcal{H}' = \text{softmax}\left(\frac{Q_{\mathcal{H}} K_{\mathcal{P}}^T}{\sqrt{d}}\right) V_{\mathcal{P}}$, where d is the embedding dimension. This design choice enjoys three advantages, including 1) strengthened connection to prompt, 2) intact and deep flow of the original prompt tokens, and 3) better computational efficiency. VIMA decoder consists of L alternating cross-attention and self-attention layers. Finally, for ease of learning and optimization, we follow common practice ([Baker et al., 2022](#)) to map predicted action tokens to discretized poses of the robot arm.

Training. We follow the standard behavioral cloning to train our models by minimizing the negative log-likelihood of predicted actions. Concretely, for a trajectory with T steps, we minimize $\min_{\theta} \sum_{t=1}^T -\log \pi_{\theta}(a_t | \mathcal{P}, \mathcal{H})$. The entire training is conducted on an offline dataset with no access to the physics simulator. To make VIMA robust to detection inaccuracies and failures, we apply *object augmentation* by randomly injecting *false-positive* detection outputs. After training, we select model checkpoints for evaluation based on the aggregated accuracy on a held-out validation set. The evaluation involves interacting with the physics simulator. We follow the best practices to train Transformer models using the AdamW optimizer ([Loshchilov & Hutter, 2019](#)), learning rate warm-up, cosine annealing ([Loshchilov & Hutter, 2016](#)), etc. See Appendix Sec. C & D for a comprehensive listing of our model and training hyperparameters.

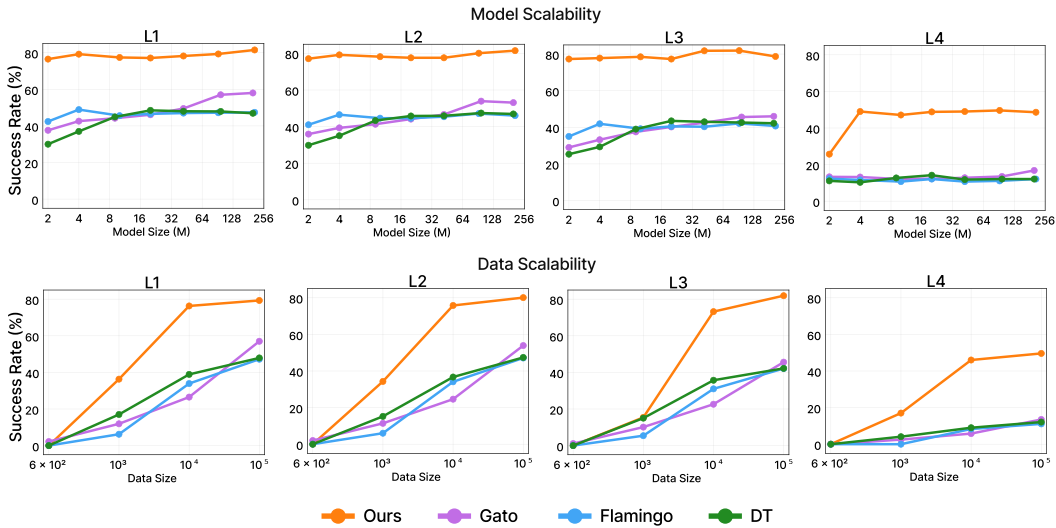


Figure 4: Scaling model and data. *Top:* We compare performance of different methods with model sizes ranging from 2M to 200M parameters. Across all model sizes and generalization levels VIMA outperforms prior works. *Bottom:* For a fixed model size of 92M parameters we compare the effect of imitation learning dataset size of 0.1%, 1%, 10%, and full imitation data. VIMA is extremely sample efficient and can achieve performance comparable to other methods with $10\times$ less data.

5 EXPERIMENTS

In this section, we aim to answer three main questions:

1. How does VIMA compare with prior SOTA transformer-based agents on a diverse collection of multimodal-prompted tasks?
2. What are the **scaling properties** of our approach in model capacity and data size?
3. How do different visual tokenizers, prompt conditioning, and prompt encoding affect decision making?

5.1 BASELINES

Gato (Reed et al., 2022) introduces a decoder-only model that solves tasks from multiple domains where tasks are specified by prompting the model with the observation and action subsequence. For fair comparison, we provide the same conditioning as VIMA, *i.e.*, our multimodal embedded prompt. Input images are divided into patches and encoded by a ViT (Dosovitskiy et al., 2020) model to produce observation tokens.

Flamingo (Alayrac et al., 2022) is a vision-language model that learns to generate textual completion in response to multimodal prompts. It embeds a variable number of prompt images into a fixed number of tokens via the Perceiver Resampler module, and conditions the language decoder on the encoded prompt by cross-attention. Flamingo does not work with embodied agents out of the box. We adapt it to support decision-masking by replacing the output layer with robot action heads.

Decision Transformer (DT) (Chen et al., 2021; Janner et al., 2021) is among the first works to reinterpret the RL problem as transformer sequence modeling. In visual RL domains like Atari games, DT is prompted on the desired reward value and outputs actions autoregressively given the RGB observation embedding. We replace DT’s initial reward prompt with our multimodal task prompt embeddings, and remove all subsequent reward tokens.

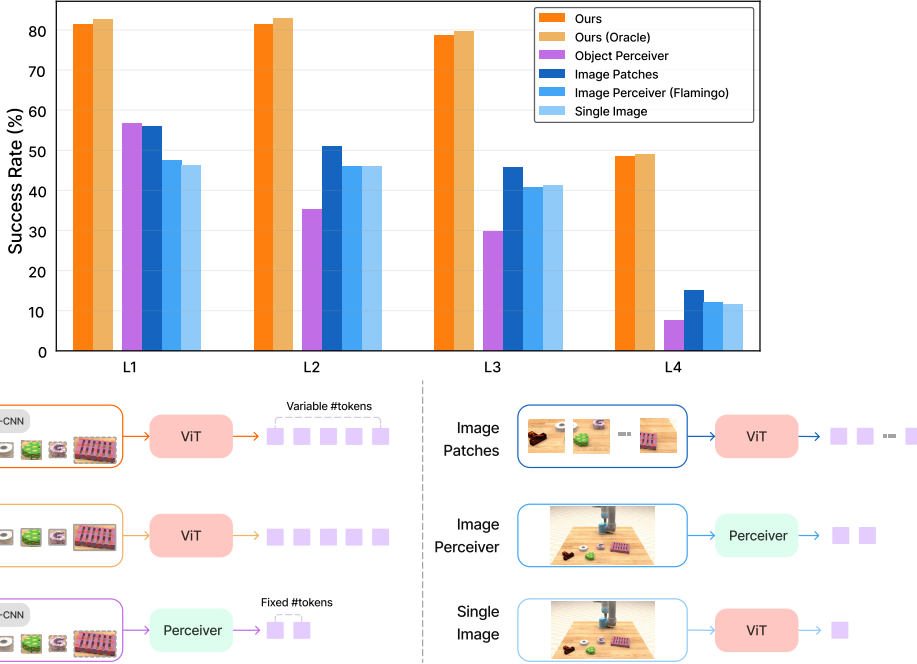


Figure 5: **Ablation on visual tokenizers.** We compare the performance of VIMA-200M model across different visual tokenizers. Our proposed object tokens outperform all methods that learn directly from raw pixels, and *Object Perceiver* that downsamples the object sequence to a fixed number of tokens.

5.2 EVALUATION RESULTS

We compare VIMA against other SOTA methods on the four levels of generalization provided in our benchmark for different model and training dataset sizes.

Model scaling. We train all methods for a spectrum of model capacities from 2M to 200M parameters, evenly spaced on the log scale. The encoder size is kept constant (pretrained T5-Base) for all methods and excluded from the parameter count. Across *all* levels of zero-shot generalization, we find that VIMA strongly outperforms prior work. Although models like Gato and Flamingo show improved performance with bigger model sizes, VIMA consistently achieves superior performance over *all* model sizes. We note that this can only be achieved with *both* cross-attention and object token sequence representation — altering any component will degrade the performance significantly, especially in the low model capacity regime (ablations in Sec. 5.3).

Data scaling. Next we investigate how different methods scale with varying dataset sizes. We compare model performance at 0.1%, 1%, 10% and full imitation learning dataset provided in VIMA-BENCH (Fig. 4). VIMA is extremely sample efficient and with just 1% of the data can achieve performance similar to baseline methods trained with 10× more data for L1 and L2 levels of generalization. In fact, for L4 we find that with just 1% of training data, VIMA already outperforms prior work trained with *entire* dataset. Finally, across all levels with just 10% of the data, VIMA can outperform prior work trained with the full dataset by a significant margin. We hypothesize that the data efficiency can be attributed to VIMA’s object-centric representation, which is less prone to overfitting than learning directly from pixels in the low-data regime. This is consistent with findings from [Sax et al. \(2018\)](#), which demonstrates that embodied agents conditioned on mid-level visual representations tend to be significantly more sample-efficient than end-to-end control from raw pixels.

Progressive Generalization. Finally, we compare the relative degradation in performance as we test the models on progressively challenging zero-shot evaluation levels without further finetuning (Fig. 6). Our method exhibits a minimal performance regression, especially between *L1* → *L2* and

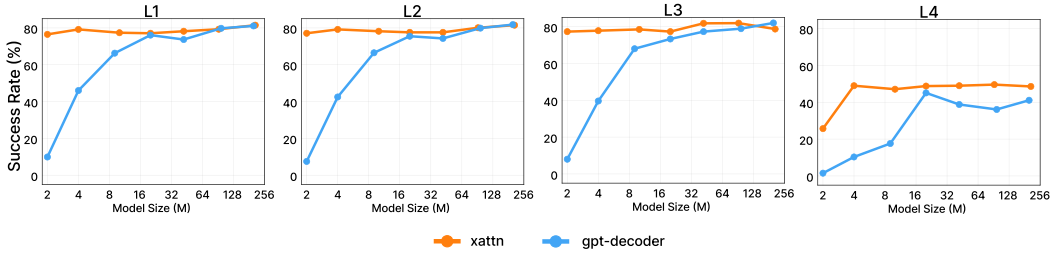


Figure 7: **Ablation: Prompt conditioning.** We compare our method (*xattn*: cross-attention prompt conditioning) with a vanilla transformer decoder (*gpt-decoder*) across different model sizes. Cross-attention is especially helpful in low-parameter regime and for harder generalization tasks.

L1 → L3. In contrast, other methods can degrade as much as 20%, particularly in the more difficult generalization testing scenarios. Although all methods degrade significantly when evaluated on *L4* (*Novel Tasks*), the drop in performance for VIMA is only *half* as severe as all other baselines. This results suggest that VIMA has developed more generalizable policy and robust representations than the competing approaches.

5.3 ABLATION STUDIES

Through extensive experiments, we ablate different design choices in VIMA and study their impact on robot decision making. We focus on the following 3 aspects: visual tokenization, prompt encoding, and prompt conditioning variants.

Visual tokenization. As explained in Sec. 4, VIMA processes the prompt and observation images into a variable number of object tokens with an off-the-shelf Mask R-CNN implementation. How important is this particular choice of visual tokenizer? We study 5 different variants and empirically evaluate their 4 levels of generalization performance on VIMA-BENCH. (1) **Ours (Oracle):** instead of using Mask R-CNN, we directly read out the groundtruth bounding box from the simulator. In other words, we use a perfect object detector to estimate the upper bound on the performance of this study; (2) **Object Perceiver:** we apply a Perceiver module (Jaegle et al., 2021b;a) to convert the variable number of objects detected in each frame to a *fixed* number of tokens. Perceiver is more computationally efficient because it reduces the average sequence length; (3) **Image Perceiver:** the same architecture as the *Perceiver Resampler* in Flamingo, which converts an image to a small, fixed number of tokens; (4) **Image patches:** following Gato, we divide an RGB frame into square patches, and extract ViT embedding tokens. The number of patches is more than the output of Image Perceiver; (5) **Single image:** Decision Transformer’s tokenizer, which encodes one image into a single token.

Fig. 5 shows the ablation results. We highlight a few findings. First, we note that our Mask R-CNN detection pipeline (Appendix, Sec. A.20) **incurs a minimal performance loss** compared to the oracle bounding boxes, thanks to the object augmentation (Sec. 4) that boosts robustness during training. Second, tokenizing from raw pixels (Image Perceiver, patches, or single embedding) consistently underperforms our object-centric format. We hypothesize that these tokenizers have to allocate extra internal capacity to parse the objects from low-level pixels, which likely impedes learning. Sax et al. (2018) echoes our finding that using mid-level vision can greatly improve agent generalization compared to an end-to-end pipeline. Third, even though *Ours* and *Object Perceiver* both use the same object bounding box inputs, the latter is significantly worse in decision making. We conclude that it is important to pass the **variable sequence of objects directly** to the robot controller rather than downsampling to a fixed number of tokens.

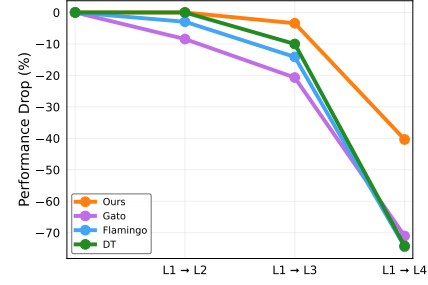


Figure 6: VIMA incurs much less performance drop than baselines as we evaluate on progressively harder zero-shot generalization.

Prompt Conditioning. VIMA conditions the robot controller (decoder) on the encoded prompt by cross-attention. A simple alternative is to concatenate the prompt \mathcal{P} and interaction history \mathcal{H} into one big sequence, and then apply a decoder-only transformer like GPT (Radford et al., 2018) to predict actions. In this ablation, we keep the object tokenizer constant, and only switch the conditioning mechanism to causal sequence modeling. Fig. 7 shows the comparison of VIMA (`xattn`) and the `gpt-decoder` variant across 4 generalization levels. While GPT achieves comparable performance in larger models, cross-attention still dominates in the small-capacity range and generalizes better in the most challenging L4 (*Novel Task*) setting. Our hypothesis is that cross-attention helps the controller stay better focused on the prompt instruction at each interaction step. This bears resemblance to the empirical results in Sanh et al. (2021); Wang et al. (2022b), which show that well-tuned encoder-decoder architectures can outperform GPT-3 in zero-shot generalization.

Prompt Encoding. We vary the size of the pre-trained T5 encoder (Raffel et al., 2020) to study the effect of prompt encoding. We experiment with three T5 model capacities: `t5-small` (30M), `t5-base` (111M), to `t5-large` (368M). For all T5 variants, we fine-tune the last two layers and freeze all other layers. We find no significant difference among the variants (Appendix, Sec. E.2), thus we set `t5-base` as default for all our models.

6 RELATED WORK

Multi-task Learning by Sequence Modeling. Transformers have enabled task unification across many AI domains (Raffel et al., 2020; Radford et al., 2019; Brown et al., 2020; Chen et al., 2022a;b; Lu et al., 2022; Wang et al., 2022c; Alayrac et al., 2022; Reed et al., 2022). For example, in **NLP**, T5 (Raffel et al., 2020) unifies all language problems into the same text-to-text format. GPT-3 (Brown et al., 2020), PaLM (Chowdhery et al., 2022), and Megatron-Turing NLG (Shoeybi et al., 2019) demonstrate emergent behaviours of intuitive task specifications by zero-shot prompting without any finetuning. In **computer vision**, Florence (Yuan et al., 2021), BiT (Kolesnikov et al., 2020), and MuST (Ghiasi et al., 2021) pre-train a shared backbone model at scale for general visual representations and transfer it across downstream vision tasks. Pix2Seq (Chen et al., 2022b) casts many vision problems into a unified sequence format. In **multimodal learning**, Flamingo (Alayrac et al., 2022), Frozen (Tsimpoukelli et al., 2021), and VL-T5 (Cho et al., 2021) design a universal API that ingests an interleaving sequence of images and text and generates free-form text. Gato (Reed et al., 2022) and HighMMT (Liang et al., 2022) are massively multi-task models across NLP, vision, and embodied agents. Our work is most similar in spirit to Gato, but we focus primarily on enabling an intuitive, multimodal prompting interface for a generalist robot agent.

Foundation Models for Embodied Agents. Foundation models (Bommasani et al., 2021; Brown et al., 2020; Raffel et al., 2020; Ramesh et al., 2022; Wei et al., 2022) have demonstrated strong emergent properties like zero-shot prompting and complex reasoning. There are many ongoing efforts to replicate this success for embodied agents, focusing on 3 aspects: 1) **Transformer agent architecture:** Decision Transformer (Chen et al., 2021; Janner et al., 2021; Zheng et al., 2022; Xu et al., 2022) and Gato (Reed et al., 2022) leverage the powerful self-attention models for sequential decision making. CLIPort (Shridhar et al., 2021) and Perceiver-Actor (Shridhar et al., 2022) apply large transformers to robot manipulation tasks. Less is More (Wang et al., 2021) generates navigation instructions from a mixture of visual landmarks and text. 2) **Pre-training for better representations:** MVP (Xiao et al., 2022), R3M (Nair et al., 2022), and Parisi et al. (2022) pre-train general visual representations for robotic perception. Li et al. (2022); Reid et al. (2022) finetune from LLM checkpoints to accelerate policy learning. MineDojo (Fan et al., 2022) and Ego4D (Grauman et al., 2021) provide large-scale multimodal databases to facilitate scalable policy training. 3) **Large language models for robot learning:** SayCan (Ahn et al., 2022) leverages the 500B PaLM (Chowdhery et al., 2022) for zero-shot concept grounding. Socratic Models (Zeng et al., 2022) composes multiple vision and language foundation models (VLMs) for multimodal reasoning in videos. Huang et al. (2022a), Inner Monologue (Huang et al., 2022b) and LM-Nav (Shah et al., 2022) successfully apply LLMs to long-horizon robot planning. VIMA differs from these works in our novel multimodal prompting formulation, which existing LLMs and VLMs do not easily support.

Robot Manipulation and Benchmarks. There are a wide range of robot manipulation tasks that require different skills and task specification formats, such as instruction following (Stepputtis et al.,

2020; Shridhar et al., 2021; Lynch & Sermanet, 2021), one-shot imitation (Finn et al., 2017; Dasari & Gupta, 2020; Duan et al., 2017), rearrangement (Batra et al., 2020; Weihs et al., 2021; Szot et al., 2021), constraint satisfaction (Brunke et al., 2021; Srinivasan et al., 2020; Thananjeyan et al., 2021), and reasoning (Shridhar et al., 2020; Gupta et al., 2019; Ahmed et al., 2021; Toyer et al., 2020; Lim et al., 2021). Multiple physics simulation benchmarks are introduced to study the above tasks. For example, iGibson (Shen et al., 2020; Li et al., 2021; Srivastava et al., 2021) simulates interactive household scenarios. Ravens (Zeng et al., 2020) and Robosuite (Zhu et al., 2020; Fan et al., 2021) design various tabletop manipulation tasks with realistic robot arms. Our VIMA-BENCH is the first robot learning benchmark to support multimodal-prompted tasks. We also standardize the evaluation protocol to systematically measure an agent’s generalization capabilities.

A more extended literature review can be found in Appendix, Sec. F.

7 CONCLUSION

Similar to GPT-3, a generalist robot agent should have an intuitive and expressive interface for human users to convey their intent. In this work, we introduce a novel *multimodal* prompting formulation that converts diverse robot manipulation tasks into a uniform sequence modeling problem. We propose VIMA, a conceptually simple transformer-based agent capable of solving tasks like visual goal, one-shot video imitation, and novel concept grounding with a single model. VIMA exhibits superior model and data scaling properties, and provides a strong starting point for future work.

8 ACKNOWLEDGEMENTS

We are extremely grateful to Shyamal Buch, Jonathan Tremblay, Ajay Mandlekar, Chris Choy, De-An Huang, Silvio Savarese, Fei Xia, Josiah Wong, Abhishek Joshi, Soroush Nasiriany, and many other colleagues and friends for their helpful feedback and insightful discussions. NVIDIA provides the necessary computing resource and infrastructure for this project. This work is done during Yunfan Jiang and Guanzhi Wang’s internships at NVIDIA. Guanzhi Wang is supported by the Kortschak fellowship in Computing and Mathematical Sciences at Caltech.

REFERENCES

- Josh Abramson, Arun Ahuja, Iain Barr, Arthur Brussee, Federico Carnevale, Mary Cassin, Rachita Chhaparia, Stephen Clark, Bogdan Damoc, Andrew Dudzik, Petko Georgiev, Aurelia Guy, Tim Harley, Felix Hill, Alden Hung, Zachary Kenton, Jessica Landon, Timothy Lillicrap, Kory Mathewson, Soňa Mokrá, Alistair Muldal, Adam Santoro, Nikolay Savinov, Vikrant Varma, Greg Wayne, Duncan Williams, Nathaniel Wong, Chen Yan, and Rui Zhu. Imitating interactive intelligence. *arXiv preprint arXiv: Arxiv-2012.05672*, 2020.
- Bernardo Aceituno, Alberto Rodriguez, Shubham Tulsiani, Abhinav Gupta, and Mustafa Mukadam. A differentiable recipe for learning visual non-prehensile planar manipulation. In *5th Annual Conference on Robot Learning*, 2021. URL <https://openreview.net/forum?id=f7KaqYLO3iE>.
- Pulkit Agrawal. The task specification problem. In Aleksandra Faust, David Hsu, and Gerhard Neumann (eds.), *Proceedings of the 5th Conference on Robot Learning*, volume 164 of *Proceedings of Machine Learning Research*, pp. 1745–1751. PMLR, 08-11 Nov 2022. URL <https://proceedings.mlr.press/v164/agrawal22a.html>.
- Ossama Ahmed, Frederik Träuble, Anirudh Goyal, Alexander Neitz, Manuel Wuthrich, Yoshua Bengio, Bernhard Schölkopf, and Stefan Bauer. Causalworld: A robotic manipulation benchmark for causal structure and transfer learning. In *9th International Conference on Learning Representations, ICLR 2021, Virtual Event, Austria, May 3-7, 2021*. OpenReview.net, 2021. URL <https://openreview.net/forum?id=SK7A5pdrgov>.
- Michael Ahn, Anthony Brohan, Noah Brown, Yevgen Chebotar, Omar Cortes, Byron David, Chelsea Finn, Keerthana Gopalakrishnan, Karol Hausman, Alex Herzog, Daniel Ho, Jasmine Hsu, Julian Ibarz, Brian Ichter, Alex Irpan, Eric Jang, Rosario Jauregui Ruano, Kyle Jeffrey, Sally Jesmonth,

Nikhil J Joshi, Ryan Julian, Dmitry Kalashnikov, Yuheng Kuang, Kuang-Huei Lee, Sergey Levine, Yao Lu, Linda Luu, Carolina Parada, Peter Pastor, Jornell Quiambao, Kanishka Rao, Jarek Rettinghouse, Diego Reyes, Pierre Sermanet, Nicolas Sievers, Clayton Tan, Alexander Toshev, Vincent Vanhoucke, Fei Xia, Ted Xiao, Peng Xu, Sichun Xu, and Mengyuan Yan. Do as i can, not as i say: Grounding language in robotic affordances. *arXiv preprint arXiv: Arxiv-2204.01691*, 2022.

Jean-Baptiste Alayrac, Jeff Donahue, Pauline Luc, Antoine Miech, Iain Barr, Yana Hasson, Karel Lenc, Arthur Mensch, Katie Millican, Malcolm Reynolds, Roman Ring, Eliza Rutherford, Serkan Cabi, Tengda Han, Zhitao Gong, Sina Samangooei, Marianne Monteiro, Jacob Menick, Sebastian Borgeaud, Andrew Brock, Aida Nematzadeh, Sahand Sharifzadeh, Mikolaj Binkowski, Ricardo Barreira, Oriol Vinyals, Andrew Zisserman, and Karen Simonyan. Flamingo: a visual language model for few-shot learning. *arXiv preprint arXiv: Arxiv-2204.14198*, 2022.

Bowen Baker, Ilge Akkaya, Peter Zhokhov, Joost Huizinga, Jie Tang, Adrien Ecoffet, Brandon Houghton, Raul Sampedro, and Jeff Clune. Video pretraining (vpt): Learning to act by watching unlabeled online videos. *arXiv preprint arXiv: Arxiv-2206.11795*, 2022.

Dhruv Batra, Angel X. Chang, Sonia Chernova, Andrew J. Davison, Jia Deng, Vladlen Koltun, Sergey Levine, Jitendra Malik, Igor Mordatch, Roozbeh Mottaghi, Manolis Savva, and Hao Su. Rearrangement: A challenge for embodied ai. *arXiv preprint arXiv: Arxiv-2011.01975*, 2020.

Homanga Bharadhwaj, Aviral Kumar, Nicholas Rhinehart, Sergey Levine, Florian Shkurti, and Animesh Garg. Conservative safety critics for exploration. In *9th International Conference on Learning Representations, ICLR 2021, Virtual Event, Austria, May 3-7, 2021*. OpenReview.net, 2021. URL <https://openreview.net/forum?id=iaO86DUuKi>.

Rishi Bommasani, Drew A. Hudson, Ehsan Adeli, Russ Altman, Simran Arora, Sydney von Arx, Michael S. Bernstein, Jeannette Bohg, Antoine Bosselut, Emma Brunskill, Erik Brynjolfsson, Shyamal Buch, Dallas Card, Rodrigo Castellon, Niladri Chatterji, Annie Chen, Kathleen Creel, Jared Quincy Davis, Dora Demszky, Chris Donahue, Moussa Doumbouya, Esin Durmus, Stefano Ermon, John Etchemendy, Kawin Ethayarajh, Li Fei-Fei, Chelsea Finn, Trevor Gale, Lauren Gillespie, Karan Goel, Noah Goodman, Shelby Grossman, Neel Guha, Tatsunori Hashimoto, Peter Henderson, John Hewitt, Daniel E. Ho, Jenny Hong, Kyle Hsu, Jing Huang, Thomas Icard, Saahil Jain, Dan Jurafsky, Pratyusha Kalluri, Siddharth Karamcheti, Geoff Keeling, Fereshte Khanl, Omar Khattab, Pang Wei Koh, Mark Krass, Ranjay Krishna, Rohith Kuditipudi, Ananya Kumar, Faisal Ladhak, Mina Lee, Tony Lee, Jure Leskovec, Isabelle Levent, Xiang Lisa Li, Xuechen Li, Tengyu Ma, Ali Malik, Christopher D. Manning, Suvir Mirchandani, Eric Mitchell, Zanele Munyikwa, Suraj Nair, Avanika Narayan, Deepak Narayanan, Ben Newman, Allen Nie, Juan Carlos Niebles, Hamed Nilforoshan, Julian Nyarko, Giray Ogut, Laurel Orr, Isabel Papadimitriou, Joon Sung Park, Chris Piech, Eva Portelance, Christopher Potts, Aditi Raghunathan, Rob Reich, Hongyu Ren, Frieda Rong, Yusuf Roohani, Camilo Ruiz, Jack Ryan, Christopher Ré, Dorsa Sadigh, Shiori Sagawa, Keshav Santhanam, Andy Shih, Krishnan Srinivasan, Alex Tamkin, Rohan Taori, Armin W. Thomas, Florian Tramèr, Rose E. Wang, William Wang, Bohan Wu, Jiajun Wu, Yuhuai Wu, Sang Michael Xie, Michihiro Yasunaga, Jiaxuan You, Matei Zaharia, Michael Zhang, Tianyi Zhang, Xikun Zhang, Yuhui Zhang, Lucia Zheng, Kaitlyn Zhou, and Percy Liang. On the opportunities and risks of foundation models. *arXiv preprint arXiv: Arxiv-2108.07258*, 2021.

Tom B. Brown, Benjamin Mann, Nick Ryder, Melanie Subbiah, Jared Kaplan, Prafulla Dhariwal, Arvind Neelakantan, Pranav Shyam, Girish Sastry, Amanda Askell, Sandhini Agarwal, Ariel Herbert-Voss, Gretchen Krueger, Tom Henighan, Rewon Child, Aditya Ramesh, Daniel M. Ziegler, Jeffrey Wu, Clemens Winter, Christopher Hesse, Mark Chen, Eric Sigler, Mateusz Litwin, Scott Gray, Benjamin Chess, Jack Clark, Christopher Berner, Sam McCandlish, Alec Radford, Ilya Sutskever, and Dario Amodei. Language models are few-shot learners. In Hugo Larochelle, Marc'Aurelio Ranzato, Raia Hadsell, Maria-Florina Balcan, and Hsuan-Tien Lin (eds.), *Advances in Neural Information Processing Systems 33: Annual Conference on Neural Information Processing Systems 2020, NeurIPS 2020, December 6-12, 2020, virtual*, volume 33, pp. 1877–1901, 2020. URL <https://proceedings.neurips.cc/paper/2020/hash/1457c0d6bfcb4967418bfb8ac142f64a-Abstract.html>.

-
- Lukas Brunke, Melissa Greeff, Adam W. Hall, Zhaocong Yuan, Siqi Zhou, Jacopo Panerati, and Angela P. Schoellig. Safe learning in robotics: From learning-based control to safe reinforcement learning. *arXiv preprint arXiv: Arxiv-2108.06266*, 2021.
- Shyamal Buch, Cristóbal Eyzaguirre, Adrien Gaidon, Jiajun Wu, Li Fei-Fei, and Juan Carlos Niebles. Revisiting the "video" in video-language understanding. *CVPR*, 2022.
- Arthur Bucker, Luis Figueiredo, Sami Haddadin, Ashish Kapoor, Shuang Ma, Sai Vemprala, and Rogerio Bonatti. Latte: Language trajectory transformer. *arXiv preprint arXiv: Arxiv-2208.02918*, 2022.
- Lili Chen, Kevin Lu, Aravind Rajeswaran, Kimin Lee, Aditya Grover, Michael Laskin, Pieter Abbeel, Aravind Srinivas, and Igor Mordatch. Decision transformer: Reinforcement learning via sequence modeling. In Marc’Aurelio Ranzato, Alina Beygelzimer, Yann N. Dauphin, Percy Liang, and Jennifer Wortman Vaughan (eds.), *Advances in Neural Information Processing Systems 34: Annual Conference on Neural Information Processing Systems 2021, NeurIPS 2021, December 6-14, 2021, virtual*, pp. 15084–15097, 2021. URL <https://proceedings.neurips.cc/paper/2021/hash/7f489f642a0ddb10272b5c31057f0663-Abstract.html>.
- Ting Chen, Saurabh Saxena, Lala Li, David J. Fleet, and Geoffrey E. Hinton. Pix2seq: A language modeling framework for object detection. In *The Tenth International Conference on Learning Representations, ICLR 2022, Virtual Event, April 25-29, 2022*. OpenReview.net, 2022a. URL <https://openreview.net/forum?id=e42KbIw6Wb>.
- Ting Chen, Saurabh Saxena, Lala Li, Tsung-Yi Lin, David J. Fleet, and Geoffrey Hinton. A unified sequence interface for vision tasks. *arXiv preprint arXiv: Arxiv-2206.07669*, 2022b.
- Jaemin Cho, Jie Lei, Hao Tan, and Mohit Bansal. Unifying vision-and-language tasks via text generation. In Marina Meila and Tong Zhang (eds.), *Proceedings of the 38th International Conference on Machine Learning, ICML 2021, 18-24 July 2021, Virtual Event*, volume 139 of *Proceedings of Machine Learning Research*, pp. 1931–1942. PMLR, 2021. URL <http://proceedings.mlr.press/v139/cho21a.html>.
- Aakanksha Chowdhery, Sharan Narang, Jacob Devlin, Maarten Bosma, Gaurav Mishra, Adam Roberts, Paul Barham, Hyung Won Chung, Charles Sutton, Sebastian Gehrmann, Parker Schuh, Kensen Shi, Sasha Tsvyashchenko, Joshua Maynez, Abhishek Rao, Parker Barnes, Yi Tay, Noam Shazeer, Vinodkumar Prabhakaran, Emily Reif, Nan Du, Ben Hutchinson, Reiner Pope, James Bradbury, Jacob Austin, Michael Isard, Guy Gur-Ari, Pengcheng Yin, Toju Duke, Anselm Levskaya, Sanjay Ghemawat, Sunipa Dev, Henryk Michalewski, Xavier Garcia, Vedant Misra, Kevin Robinson, Liam Fedus, Denny Zhou, Daphne Ippolito, David Luan, Hyeontaek Lim, Barret Zoph, Alexander Spiridonov, Ryan Sepassi, David Dohan, Shivani Agrawal, Mark Omernick, Andrew M. Dai, Thanumalayan Sankaranarayana Pillai, Marie Pellat, Aitor Lewkowycz, Erica Moreira, Rewon Child, Oleksandr Polozov, Katherine Lee, Zongwei Zhou, Xuezhi Wang, Brennan Saeta, Mark Diaz, Orhan Firat, Michele Catasta, Jason Wei, Kathy Meier-Hellstern, Douglas Eck, Jeff Dean, Slav Petrov, and Noah Fiedel. Palm: Scaling language modeling with pathways. *arXiv preprint arXiv: Arxiv-2204.02311*, 2022.
- Jack Collins, Shelvin Chand, Anthony Vanderkop, and David Howard. A review of physics simulators for robotic applications. *IEEE Access*, 9:51416–51431, 2021.
- Erwin Coumans and Yunfei Bai. Pybullet, a python module for physics simulation for games, robotics and machine learning. <http://pybullet.org>, 2016–2021.
- Sudeep Dasari and Abhinav Gupta. Transformers for one-shot visual imitation. In Jens Kober, Fabio Ramos, and Claire J. Tomlin (eds.), *4th Conference on Robot Learning, CoRL 2020, 16-18 November 2020, Virtual Event / Cambridge, MA, USA*, volume 155 of *Proceedings of Machine Learning Research*, pp. 2071–2084. PMLR, 2020. URL <https://proceedings.mlr.press/v155/dasari21a.html>.
- Matt Deitke, Eli VanderBilt, Alvaro Herrasti, Luca Weihs, Jordi Salvador, Kiana Ehsani, Winson Han, Eric Kolve, Ali Farhadi, Aniruddha Kembhavi, and Roozbeh Mottaghi. Procthor: Large-scale embodied ai using procedural generation. *arXiv preprint arXiv: Arxiv-2206.06994*, 2022.

Alexey Dosovitskiy, Lucas Beyer, Alexander Kolesnikov, Dirk Weissenborn, Xiaohua Zhai, Thomas Unterthiner, Mostafa Dehghani, Matthias Minderer, Georg Heigold, Sylvain Gelly, Jakob Uszkoreit, and Neil Houlsby. An image is worth 16x16 words: Transformers for image recognition at scale. *arXiv preprint arXiv: Arxiv-2010.11929*, 2020.

Laura Downs, Anthony Francis, Nate Koenig, Brandon Kinman, Ryan Hickman, Krista Reymann, Thomas B McHugh, and Vincent Vanhoucke. Google scanned objects: A high-quality dataset of 3d scanned household items. *arXiv preprint arXiv:2204.11918*, 2022.

Jiafei Duan, Samson Yu, Hui Li Tan, Hongyuan Zhu, and Cheston Tan. A survey of embodied AI: from simulators to research tasks. *IEEE Trans. Emerg. Top. Comput. Intell.*, 6(2):230–244, 2022. doi: 10.1109/TETCI.2022.3141105. URL <https://doi.org/10.1109/TETCI.2022.3141105>.

Yan Duan, Marcin Andrychowicz, Bradly C. Stadie, Jonathan Ho, Jonas Schneider, Ilya Sutskever, Pieter Abbeel, and Wojciech Zaremba. One-shot imitation learning. In Isabelle Guyon, Ulrike von Luxburg, Samy Bengio, Hanna M. Wallach, Rob Fergus, S. V. N. Vishwanathan, and Roman Garnett (eds.), *Advances in Neural Information Processing Systems 30: Annual Conference on Neural Information Processing Systems 2017, December 4-9, 2017, Long Beach, CA, USA*, pp. 1087–1098, 2017. URL <https://proceedings.neurips.cc/paper/2017/hash/ba3866600c3540f67c1e9575e213be0a-Abstract.html>.

Kiana Ehsani, Winson Han, Alvaro Herrasti, Eli VanderBilt, Luca Weihs, Eric Kolve, Aniruddha Kembhavi, and Roozbeh Mottaghi. Manipulathor: A framework for visual object manipulation. In *Proceedings of the IEEE/CVF Conference on Computer Vision and Pattern Recognition (CVPR)*, pp. 4497–4506, June 2021.

Linxi Fan, Yuke Zhu, Jiren Zhu, Zihua Liu, Orien Zeng, Anchit Gupta, Joan Creus-Costa, Silvio Savarese, and Li Fei-Fei. Surreal: Open-source reinforcement learning framework and robot manipulation benchmark. In Aude Billard, Anca Dragan, Jan Peters, and Jun Morimoto (eds.), *Proceedings of The 2nd Conference on Robot Learning*, volume 87 of *Proceedings of Machine Learning Research*, pp. 767–782. PMLR, 29-31 Oct 2018. URL <https://proceedings.mlr.press/v87/fan18a.html>.

Linxi Fan, Yuke Zhu, Jiren Zhu, Zihua Liu, Orien Zeng, Anchit Gupta, Joan Creus-Costa, Silvio Savarese, and Li Fei-Fei. Surreal-system: Fully-integrated stack for distributed deep reinforcement learning. *arXiv preprint arXiv: Arxiv-1909.12989*, 2019.

Linxi Fan, Guanzhi Wang, De-An Huang, Zhiding Yu, Li Fei-Fei, Yuke Zhu, and Animashree Anandkumar. SECANT: self-expert cloning for zero-shot generalization of visual policies. In Marina Meila and Tong Zhang (eds.), *Proceedings of the 38th International Conference on Machine Learning, ICML 2021, 18-24 July 2021, Virtual Event*, volume 139 of *Proceedings of Machine Learning Research*, pp. 3088–3099. PMLR, 2021. URL <http://proceedings.mlr.press/v139/fan21c.html>.

Linxi Fan, Guanzhi Wang, Yunfan Jiang, Ajay Mandlekar, Yuncong Yang, Haoyi Zhu, Andrew Tang, De-An Huang, Yuke Zhu, and Anima Anandkumar. Minedojo: Building open-ended embodied agents with internet-scale knowledge. *arXiv preprint arXiv: Arxiv-2206.08853*, 2022.

Chelsea Finn, Tianhe Yu, Tianhao Zhang, Pieter Abbeel, and Sergey Levine. One-shot visual imitation learning via meta-learning. *arXiv preprint arXiv: Arxiv-1709.04905*, 2017.

Tsu-Jui Fu, Linjie Li, Zhe Gan, Kevin Lin, William Yang Wang, Lijuan Wang, and Zicheng Liu. Violet : End-to-end video-language transformers with masked visual-token modeling. *arXiv preprint arXiv: Arxiv-2111.12681*, 2021.

Chuang Gan, Siyuan Zhou, Jeremy Schwartz, Seth Alter, Abhishek Bhandwaldar, Dan Gutfreund, Daniel L. K. Yamins, James J DiCarlo, Josh McDermott, Antonio Torralba, and Joshua B. Tenenbaum. The threeeworld transport challenge: A visually guided task-and-motion planning benchmark for physically realistic embodied ai. *arXiv preprint arXiv: Arxiv-2103.14025*, 2021.

Golnaz Ghiasi, Barret Zoph, Ekin D. Cubuk, Quoc V. Le, and Tsung-Yi Lin. Multi-task self-training for learning general representations. In *2021 IEEE/CVF International Conference on Computer Vision, ICCV 2021, Montreal, QC, Canada, October 10-17, 2021*, pp. 8836–8845. IEEE, 2021. doi: 10.1109/ICCV48922.2021.00873. URL <https://doi.org/10.1109/ICCV48922.2021.00873>.

Kristen Grauman, Andrew Westbury, Eugene Byrne, Zachary Chavis, Antonino Furnari, Rohit Girdhar, Jackson Hamburger, Hao Jiang, Miao Liu, Xingyu Liu, Miguel Martin, Tushar Nagarajan, Ilija Radosavovic, Santhosh Kumar Ramakrishnan, Fiona Ryan, Jayant Sharma, Michael Wray, Mengmeng Xu, Eric Zhongcong Xu, Chen Zhao, Siddhant Bansal, Dhruv Batra, Vincent Cartillier, Sean Crane, Tien Do, Morrie Doulaty, Akshay Erapalli, Christoph Feichtenhofer, Adriano Fragnomeni, Qichen Fu, Abrham Gebreselasie, Cristina Gonzalez, James Hillis, Xuhua Huang, Yifei Huang, Wenqi Jia, Leslie Khoo, Jachym Kolar, Satwik Kottur, Anurag Kumar, Federico Landini, Chao Li, Yanghao Li, Zhenqiang Li, Karttikeya Mangalam, Raghava Modhugu, Jonathan Munro, Tullie Murrell, Takumi Nishiyasu, Will Price, Paola Ruiz Puentes, Merey Ramazanova, Leda Sari, Kiran Somasundaram, Audrey Southerland, Yusuke Sugano, Ruijie Tao, Minh Vo, Yuchen Wang, Xindi Wu, Takuma Yagi, Ziwei Zhao, Yunyi Zhu, Pablo Arbelaez, David Crandall, Dima Damen, Giovanni Maria Farinella, Christian Fuegen, Bernard Ghanem, Vamsi Krishna Ithapu, C. V. Jawahar, Hanbyul Joo, Kris Kitani, Haizhou Li, Richard Newcombe, Aude Oliva, Hyun Soo Park, James M. Rehg, Yoichi Sato, Jianbo Shi, Mike Zheng Shou, Antonio Torralba, Lorenzo Torresani, Mingfei Yan, and Jitendra Malik. Ego4d: Around the world in 3,000 hours of egocentric video. *arXiv preprint arXiv: Arxiv-2110.07058*, 2021.

Abhishek Gupta, Vikash Kumar, Corey Lynch, Sergey Levine, and Karol Hausman. Relay policy learning: Solving long-horizon tasks via imitation and reinforcement learning. In Leslie Pack Kaelbling, Danica Kragic, and Komei Sugiura (eds.), *3rd Annual Conference on Robot Learning, CoRL 2019, Osaka, Japan, October 30 - November 1, 2019, Proceedings*, volume 100 of *Proceedings of Machine Learning Research*, pp. 1025–1037. PMLR, 2019. URL <http://proceedings.mlr.press/v100/gupta20a.html>.

Agrim Gupta, Linxi Fan, Surya Ganguli, and Li Fei-Fei. Metamorph: Learning universal controllers with transformers. In *International Conference on Learning Representations*, 2022. URL https://openreview.net/forum?id=Opmqtk_GvYL.

Kaiming He, Georgia Gkioxari, Piotr Dollár, and Ross Girshick. Mask r-cnn. *arXiv preprint arXiv: Arxiv-1703.06870*, 2017.

Tracy H Heibeck and Ellen M Markman. Word learning in children: An examination of fast mapping. *Child development*, pp. 1021–1034, 1987.

Karl Moritz Hermann, Felix Hill, Simon Green, Fumin Wang, Ryan Faulkner, Hubert Soyer, David Szepesvari, Wojciech Marian Czarnecki, Max Jaderberg, Denis Teplyashin, Marcus Wainwright, Chris Apps, Demis Hassabis, and Phil Blunsom. Grounded language learning in a simulated 3d world. *arXiv preprint arXiv: Arxiv-1706.06551*, 2017.

De-An Huang, Danfei Xu, Yuke Zhu, Animesh Garg, Silvio Savarese, Li Fei-Fei, and Juan Carlos Niebles. Continuous relaxation of symbolic planner for one-shot imitation learning. In *2019 IEEE/RSJ International Conference on Intelligent Robots and Systems, IROS 2019, Macau, SAR, China, November 3-8, 2019*, pp. 2635–2642. IEEE, 2019. doi: 10.1109/IROS40897.2019.8967761. URL <https://doi.org/10.1109/IROS40897.2019.8967761>.

Wenlong Huang, Pieter Abbeel, Deepak Pathak, and Igor Mordatch. Language models as zero-shot planners: Extracting actionable knowledge for embodied agents. In Kamalika Chaudhuri, Stefanie Jegelka, Le Song, Csaba Szepesvári, Gang Niu, and Sivan Sabato (eds.), *International Conference on Machine Learning, ICML 2022, 17-23 July 2022, Baltimore, Maryland, USA*, volume 162 of *Proceedings of Machine Learning Research*, pp. 9118–9147. PMLR, 2022a. URL <https://proceedings.mlr.press/v162/huang22a.html>.

Wenlong Huang, Fei Xia, Ted Xiao, Harris Chan, Jacky Liang, Pete Florence, Andy Zeng, Jonathan Tompson, Igor Mordatch, Yevgen Chebotar, Pierre Sermanet, Noah Brown, Tomas Jackson, Linda Luu, Sergey Levine, Karol Hausman, and Brian Ichter. Inner monologue: Embodied reasoning through planning with language models. *arXiv preprint arXiv: Arxiv-2207.05608*, 2022b.

Andrew Jaegle, Sebastian Borgeaud, Jean-Baptiste Alayrac, Carl Doersch, Catalin Ionescu, David Ding, Skanda Koppula, Daniel Zoran, Andrew Brock, Evan Shelhamer, Olivier Hénaff, Matthew M. Botvinick, Andrew Zisserman, Oriol Vinyals, and João Carreira. Perceiver io: A general architecture for structured inputs & outputs. *arXiv preprint arXiv: Arxiv-2107.14795*, 2021a.

Andrew Jaegle, Felix Gimeno, Andrew Brock, Andrew Zisserman, Oriol Vinyals, and Joao Carreira. Perceiver: General perception with iterative attention. *arXiv preprint arXiv: Arxiv-2103.03206*, 2021b.

Stephen James, Zicong Ma, David Rovick Arrojo, and Andrew J. Davison. Rlbench: The robot learning benchmark & learning environment. *arXiv preprint arXiv: Arxiv-1909.12271*, 2019.

Michael Janner, Qiyang Li, and Sergey Levine. Offline reinforcement learning as one big sequence modeling problem. In Marc’Aurelio Ranzato, Alina Beygelzimer, Yann N. Dauphin, Percy Liang, and Jennifer Wortman Vaughan (eds.), *Advances in Neural Information Processing Systems 34: Annual Conference on Neural Information Processing Systems 2021, NeurIPS 2021, December 6-14, 2021, virtual*, pp. 1273–1286, 2021. URL <https://proceedings.neurips.cc/paper/2021/hash/099fe6b0b444c23836c4a5d07346082b-Abstract.html>.

Salman Khan, Muzammal Naseer, Munawar Hayat, Syed Waqas Zamir, Fahad Shahbaz Khan, and Mubarak Shah. Transformers in vision: A survey. *arXiv preprint arXiv: Arxiv-2101.01169*, 2021.

Apoorv Khandelwal, Luca Weihs, Rozbeh Mottaghi, and Aniruddha Kembhavi. Simple but effective: Clip embeddings for embodied ai. *arXiv preprint arXiv: Arxiv-2111.09888*, 2021.

Iasonas Kokkinos. Ubernet: Training a ‘universal’ convolutional neural network for low-, mid-, and high-level vision using diverse datasets and limited memory. *arXiv preprint arXiv: Arxiv-1609.02132*, 2016.

Alexander Kolesnikov, Lucas Beyer, Xiaohua Zhai, Joan Puigcerver, Jessica Yung, Sylvain Gelly, and Neil Houlsby. Big transfer (bit): General visual representation learning. In Andrea Vedaldi, Horst Bischof, Thomas Brox, and Jan-Michael Frahm (eds.), *Computer Vision - ECCV 2020 - 16th European Conference, Glasgow, UK, August 23-28, 2020, Proceedings, Part V*, volume 12350 of *Lecture Notes in Computer Science*, pp. 491–507. Springer, 2020. doi: 10.1007/978-3-030-58558-7\29. URL https://doi.org/10.1007/978-3-030-58558-7_29.

Alexander Kolesnikov, André Susano Pinto, Lucas Beyer, Xiaohua Zhai, Jeremiah Harmsen, and Neil Houlsby. Uvim: A unified modeling approach for vision with learned guiding codes. *arXiv preprint arXiv: Arxiv-2205.10337*, 2022.

Chengshu Li, Fei Xia, Roberto Martín-Martín, Michael Lingelbach, Sanjana Srivastava, Bokui Shen, Kent Elliott Vainio, Cem Gokmen, Gokul Dharan, Tanish Jain, Andrey Kurenkov, C. Karen Liu, Hyowon Gweon, Jiajun Wu, Li Fei-Fei, and Silvio Savarese. igibson 2.0: Object-centric simulation for robot learning of everyday household tasks. In Aleksandra Faust, David Hsu, and Gerhard Neumann (eds.), *Conference on Robot Learning, 8-11 November 2021, London, UK*, volume 164 of *Proceedings of Machine Learning Research*, pp. 455–465. PMLR, 2021. URL <https://proceedings.mlr.press/v164/l122b.html>.

Shuang Li, Xavier Puig, Chris Paxton, Yilun Du, Clinton Wang, Linxi Fan, Tao Chen, De-An Huang, Ekin Akyürek, Anima Anandkumar, Jacob Andreas, Igor Mordatch, Antonio Torralba, and Yuke Zhu. Pre-trained language models for interactive decision-making. *arXiv preprint arXiv: Arxiv-2202.01771*, 2022.

Paul Pu Liang, Yiwei Lyu, Xiang Fan, Shentong Mo, Dani Yogatama, Louis-Philippe Morency, and Ruslan Salakhutdinov. Highmmt: Towards modality and task generalization for high-modality representation learning. *arXiv preprint arXiv: Arxiv-2203.01311*, 2022.

Michael H. Lim, Andy Zeng, Brian Ichter, Maryam Bandari, Erwin Coumans, Claire Tomlin, Stefan Schaal, and Aleksandra Faust. Multi-task learning with sequence-conditioned transporter networks. *arXiv preprint arXiv: Arxiv-2109.07578*, 2021.

-
- Tianyang Lin, Yuxin Wang, Xiangyang Liu, and Xipeng Qiu. A survey of transformers. *arXiv preprint arXiv: Arxiv-2106.04554*, 2021.
- Ziyuan Liu, Wei Liu, Yuzhe Qin, Fanbo Xiang, Minghao Gou, Songyan Xin, Maximo A Roa, Berk Calli, Hao Su, Yu Sun, et al. Ocrtoc: A cloud-based competition and benchmark for robotic grasping and manipulation. *IEEE Robotics and Automation Letters*, 7(1):486–493, 2021.
- Ilya Loshchilov and Frank Hutter. Sgdr: Stochastic gradient descent with warm restarts. *arXiv preprint arXiv: Arxiv-1608.03983*, 2016.
- Ilya Loshchilov and Frank Hutter. SGDR: stochastic gradient descent with warm restarts. In *5th International Conference on Learning Representations, ICLR 2017, Toulon, France, April 24-26, 2017, Conference Track Proceedings*. OpenReview.net, 2017. URL <https://openreview.net/forum?id=Skq89Scxx>.
- Ilya Loshchilov and Frank Hutter. Decoupled weight decay regularization. In *7th International Conference on Learning Representations, ICLR 2019, New Orleans, LA, USA, May 6-9, 2019*. OpenReview.net, 2019. URL <https://openreview.net/forum?id=Bkg6RiCqY7>.
- Jiasen Lu, Vedanuj Goswami, Marcus Rohrbach, Devi Parikh, and Stefan Lee. 12-in-1: Multi-task vision and language representation learning. In *2020 IEEE/CVF Conference on Computer Vision and Pattern Recognition, CVPR 2020, Seattle, WA, USA, June 13-19, 2020*, pp. 10434–10443. Computer Vision Foundation / IEEE, 2020. doi: 10.1109/CVPR42600.2020.01045. URL https://openaccess.thecvf.com/content_CVPR_2020/html/Lu_12-in-1_Multi-Task_Vision_and_Language_Representation_Learning_CVPR_2020_paper.html.
- Jiasen Lu, Christopher Clark, Rowan Zellers, Roozbeh Mottaghi, and Aniruddha Kembhavi. Unified-io: A unified model for vision, language, and multi-modal tasks. *arXiv preprint arXiv: Arxiv-2206.08916*, 2022.
- Corey Lynch and Pierre Sermanet. Language conditioned imitation learning over unstructured data. In Dylan A. Shell, Marc Toussaint, and M. Ani Hsieh (eds.), *Robotics: Science and Systems XVII, Virtual Event, July 12-16, 2021*, 2021. doi: 10.15607/RSS.2021.XVII.047. URL <https://doi.org/10.15607/RSS.2021.XVII.047>.
- Bryan McCann, Nitish Shirish Keskar, Caiming Xiong, and Richard Socher. The natural language decathlon: Multitask learning as question answering. *arXiv preprint arXiv: Arxiv-1806.08730*, 2018.
- Nathan Morrical, Jonathan Tremblay, Stan Birchfield, and Ingo Wald. NVISII: Nvidia scene imaging interface, 2020. <https://github.com/owl-project/NVISII/>.
- Suraj Nair, Aravind Rajeswaran, Vikash Kumar, Chelsea Finn, and Abhinav Gupta. R3m: A universal visual representation for robot manipulation. *arXiv preprint arXiv: Arxiv-2203.12601*, 2022.
- OpenAI, Christopher Berner, Greg Brockman, Brooke Chan, Vicki Cheung, Przemyslaw Debiak, Christy Dennison, David Farhi, Quirin Fischer, Shariq Hashme, Chris Hesse, Rafal Józefowicz, Scott Gray, Catherine Olsson, Jakub Pachocki, Michael Petrov, Henrique P. d. O. Pinto, Jonathan Raiman, Tim Salimans, Jeremy Schlatter, Jonas Schneider, Szymon Sidor, Ilya Sutskever, Jie Tang, Filip Wolski, and Susan Zhang. Dota 2 with large scale deep reinforcement learning. *arXiv preprint arXiv: Arxiv-1912.06680*, 2019.
- Tom Le Paine, Sergio Gómez Colmenarejo, Ziyu Wang, Scott Reed, Yusuf Aytar, Tobias Pfaff, Matt W. Hoffman, Gabriel Barth-Maron, Serkan Cabi, David Budden, and Nando de Freitas. One-shot high-fidelity imitation: Training large-scale deep nets with rl. *arXiv preprint arXiv: Arxiv-1810.05017*, 2018.
- Simone Parisi, Aravind Rajeswaran, Senthil Purushwalkam, and Abhinav Gupta. The unsurprising effectiveness of pre-trained vision models for control. In Kamalika Chaudhuri, Stefanie Jegelka, Le Song, Csaba Szepesvári, Gang Niu, and Sivan Sabato (eds.), *International Conference on Machine Learning, ICML 2022, 17-23 July 2022, Baltimore, Maryland, USA*, volume 162 of *Proceedings of Machine Learning Research*, pp. 17359–17371. PMLR, 2022. URL <https://proceedings.mlr.press/v162/parisi22a.html>.

Adam Paszke, Sam Gross, Francisco Massa, Adam Lerer, James Bradbury, Gregory Chanan, Trevor Killeen, Zeming Lin, Natalia Gimelshein, Luca Antiga, Alban Desmaison, Andreas Kopf, Edward Yang, Zachary DeVito, Martin Raison, Alykhan Tejani, Sasank Chilamkurthy, Benoit Steiner, Lu Fang, Junjie Bai, and Soumith Chintala. Pytorch: An imperative style, high-performance deep learning library. In H. Wallach, H. Larochelle, A. Beygelzimer, F. d’Alché-Buc, E. Fox, and R. Garnett (eds.), *Advances in Neural Information Processing Systems 32*, pp. 8024–8035. Curran Associates, Inc., 2019.

Xavier Puig, Kevin Ra, Marko Boben, Jiaman Li, Tingwu Wang, Sanja Fidler, and Antonio Torralba. Virtualhome: Simulating household activities via programs. In *2018 IEEE Conference on Computer Vision and Pattern Recognition, CVPR 2018, Salt Lake City, UT, USA, June 18-22, 2018*, pp. 8494–8502. Computer Vision Foundation / IEEE Computer Society, 2018. doi: 10.1109/CVPR.2018.00886. URL http://openaccess.thecvf.com/content_cvpr_2018/html/Puig_VirtualHome_Simulating_Household_CVPR_2018_paper.html.

Alec Radford, Karthik Narasimhan, Tim Salimans, and Ilya Sutskever. Improving language understanding by generative pre-training. *OpenAI*, 2018.

Alec Radford, Jeffrey Wu, Rewon Child, David Luan, Dario Amodei, Ilya Sutskever, et al. Language models are unsupervised multitask learners. *OpenAI blog*, 1(8):9, 2019.

Alec Radford, Jong Wook Kim, Chris Hallacy, Aditya Ramesh, Gabriel Goh, Sandhini Agarwal, Girish Sastry, Amanda Askell, Pamela Mishkin, Jack Clark, et al. Learning transferable visual models from natural language supervision. In *International Conference on Machine Learning*, pp. 8748–8763. PMLR, 2021.

Colin Raffel, Noam Shazeer, Adam Roberts, Katherine Lee, Sharan Narang, Michael Matena, Yanqi Zhou, Wei Li, and Peter J. Liu. Exploring the limits of transfer learning with a unified text-to-text transformer. *J. Mach. Learn. Res.*, 21:140:1–140:67, 2020. URL <http://jmlr.org/papers/v21/20-074.html>.

Aditya Ramesh, Prafulla Dhariwal, Alex Nichol, Casey Chu, and Mark Chen. Hierarchical text-conditional image generation with clip latents. *arXiv preprint arXiv: Arxiv-2204.06125*, 2022.

Harish Ravichandar, Athanasios S Polydoros, Sonia Chernova, and Aude Billard. Recent advances in robot learning from demonstration. *Annual review of control, robotics, and autonomous systems*, 3: 297–330, 2020.

Scott Reed, Konrad Zolna, Emilio Parisotto, Sergio Gomez Colmenarejo, Alexander Novikov, Gabriel Barth-Maron, Mai Gimenez, Yury Sulsky, Jackie Kay, Jost Tobias Springenberg, Tom Eccles, Jake Bruce, Ali Razavi, Ashley Edwards, Nicolas Heess, Yutian Chen, Raia Hadsell, Oriol Vinyals, Mahyar Bordbar, and Nando de Freitas. A generalist agent. *arXiv preprint arXiv: Arxiv-2205.06175*, 2022.

Machel Reid, Yutaro Yamada, and Shixiang Shane Gu. Can wikipedia help offline reinforcement learning? *arXiv preprint arXiv: Arxiv-2201.12122*, 2022.

Victor Sanh, Albert Webson, Colin Raffel, Stephen H. Bach, Lintang A. Sutawika, Zaid Alyafeai, Antoine Chaffin, Arnaud Stiegler, Teven Le Scao, Arun Raja, Manan Dey, M Saiful Bari, Canwen Xu, Urmish Thakker, Shanya Sharma, Eliza Szczechla, Taewoon Kim, Gunjan Chhablani, Nihal V. Nayak, Debajyoti Datta, Jonathan Chang, Mike Tian-Jian Jiang, Han Wang, Matteo Manica, Sheng Shen, Zheng Xin Yong, Harshit Pandey, Rachel Bawden, Thomas Wang, Trishala Neeraj, Jos Rozen, Abheesht Sharma, Andrea Santilli, Thibault Févry, Jason Alan Fries, Ryan Teehan, Stella Rose Biderman, Leo Gao, T. Bers, Thomas Wolf, and Alexander M. Rush. Multitask prompted training enables zero-shot task generalization. *Iclr*, 2021.

Manolis Savva, Abhishek Kadian, Oleksandr Maksymets, Yili Zhao, Erik Wijmans, Bhavana Jain, Julian Straub, Jia Liu, Vladlen Koltun, Jitendra Malik, Devi Parikh, and Dhruv Batra. Habitat: A platform for embodied ai research. In *Proceedings of the IEEE/CVF International Conference on Computer Vision (ICCV)*, October 2019.

-
- Alexander Sax, Bradley Emi, Amir R. Zamir, Leonidas Guibas, Silvio Savarese, and Jitendra Malik. Mid-level visual representations improve generalization and sample efficiency for learning visuomotor policies. *arXiv preprint arXiv: Arxiv-1812.11971*, 2018.
- Dhruv Shah, Blazej Osinski, Brian Ichter, and Sergey Levine. Lm-nav: Robotic navigation with large pre-trained models of language, vision, and action. *arXiv preprint arXiv: Arxiv-2207.04429*, 2022.
- Noam Shazeer. Glu variants improve transformer. *arXiv preprint arXiv: Arxiv-2002.05202*, 2020.
- Bokui Shen, Fei Xia, Chengshu Li, Roberto Martín-Martín, Linxi Fan, Guanzhi Wang, Claudia Pérez-D'Arpino, Shyamal Buch, Sanjana Srivastava, Lyne P. Tchapmi, Micael E. Tchapmi, Kent Vainio, Josiah Wong, Li Fei-Fei, and Silvio Savarese. igibson 1.0: a simulation environment for interactive tasks in large realistic scenes. *arXiv preprint arXiv: Arxiv-2012.02924*, 2020.
- Tianlin Tim Shi, Andrej Karpathy, Linxi Jim Fan, Jonathan Hernandez, and Percy Liang. World of bits: an open-domain platform for web-based agents. *ICML*, 2017. URL <https://dl.acm.org/doi/10.5555/3305890.3306005>.
- Mohammad Shoeybi, Mostafa Patwary, Raul Puri, Patrick LeGresley, Jared Casper, and Bryan Catanzaro. Megatron-lm: Training multi-billion parameter language models using model parallelism. *arXiv preprint arXiv:1909.08053*, 2019.
- Mohit Shridhar, Jesse Thomason, Daniel Gordon, Yonatan Bisk, Winson Han, Roozbeh Mottaghi, Luke Zettlemoyer, and Dieter Fox. ALFRED: A benchmark for interpreting grounded instructions for everyday tasks. In *2020 IEEE/CVF Conference on Computer Vision and Pattern Recognition, CVPR 2020, Seattle, WA, USA, June 13-19, 2020*, pp. 10737–10746. Computer Vision Foundation / IEEE, 2020. doi: 10.1109/CVPR42600.2020.01075. URL https://openaccess.thecvf.com/content_CVPR_2020/html/Shridhar_ALFRED_A_Benchmark_for_Interpreting_Grounded_Instructions_for_Everyday_Tasks_CVPR_2020_paper.html.
- Mohit Shridhar, Lucas Manuelli, and Dieter Fox. Cliport: What and where pathways for robotic manipulation. *arXiv preprint arXiv: Arxiv-2109.12098*, 2021.
- Mohit Shridhar, Lucas Manuelli, and Dieter Fox. Perceiver-actor: A multi-task transformer for robotic manipulation. *arXiv preprint arXiv: Arxiv-2209.05451*, 2022.
- Krishnan Srinivasan, Benjamin Eysenbach, Sehoon Ha, Jie Tan, and Chelsea Finn. Learning to be safe: Deep rl with a safety critic. *arXiv preprint arXiv: Arxiv-2010.14603*, 2020.
- Sanjana Srivastava, Chengshu Li, Michael Lingelbach, Roberto Martín-Martín, Fei Xia, Kent Elliott Vainio, Zheng Lian, Cem Gokmen, Shyamal Buch, C. Karen Liu, Silvio Savarese, Hyowon Gweon, Jiajun Wu, and Li Fei-Fei. BEHAVIOR: benchmark for everyday household activities in virtual, interactive, and ecological environments. In Aleksandra Faust, David Hsu, and Gerhard Neumann (eds.), *Conference on Robot Learning, 8-11 November 2021, London, UK*, volume 164 of *Proceedings of Machine Learning Research*, pp. 477–490. PMLR, 2021. URL <https://proceedings.mlr.press/v164/srivastava22a.html>.
- Elias Stengel-Eskin, Andrew Hundt, Zhuohong He, Aditya Murali, Nakul Gopalan, Matthew Gombolay, and Gregory Hager. Guiding multi-step rearrangement tasks with natural language instructions. In Aleksandra Faust, David Hsu, and Gerhard Neumann (eds.), *Proceedings of the 5th Conference on Robot Learning*, volume 164 of *Proceedings of Machine Learning Research*, pp. 1486–1501. PMLR, 08–11 Nov 2022. URL <https://proceedings.mlr.press/v164/stengel-eskin22a.html>.
- Simon Stepputtis, Joseph Campbell, Mariano Phiellipp, Stefan Lee, Chitta Baral, and Heni Ben Amor. Language-Conditioned Imitation Learning for Robot Manipulation Tasks, October 2020. URL <http://arxiv.org/abs/2010.12083>. arXiv:2010.12083 [cs].
- Andrew Szot, Alexander Clegg, Eric Undersander, Erik Wijmans, Yili Zhao, John Turner, Noah Maestre, Mustafa Mukadam, Devendra Singh Chaplot, Oleksandr Maksymets, Aaron Gokaslan, Vladimir Vondrus, Sameer Dharur, Franziska Meier, Wojciech Galuba, Angel X.

Chang, Zsolt Kira, Vladlen Koltun, Jitendra Malik, Manolis Savva, and Dhruv Batra. Habitat 2.0: Training home assistants to rearrange their habitat. In Marc’Aurelio Ranzato, Alina Beygelzimer, Yann N. Dauphin, Percy Liang, and Jennifer Wortman Vaughan (eds.), *Advances in Neural Information Processing Systems 34: Annual Conference on Neural Information Processing Systems 2021, NeurIPS 2021, December 6-14, 2021, virtual*, pp. 251–266, 2021. URL <https://proceedings.neurips.cc/paper/2021/hash/021bbc7ee20b71134d53e20206bd6feb-Abstract.html>.

Yi Tay, Mostafa Dehghani, Dara Bahri, and Donald Metzler. Efficient transformers: A survey. *arXiv preprint arXiv: Arxiv-2009.06732*, 2020.

Open Ended Learning Team, Adam Stooke, Anuj Mahajan, Catarina Barros, Charlie Deck, Jakob Bauer, Jakub Sygnowski, Maja Trebacz, Max Jaderberg, Michael Mathieu, Nat McAleese, Nathalie Bradley-Schmieg, Nathaniel Wong, Nicolas Porcel, Roberta Raileanu, Steph Hughes-Fitt, Valentin Dalibard, and Wojciech Marian Czarnecki. Open-ended learning leads to generally capable agents. *arXiv preprint arXiv: Arxiv-2107.12808*, 2021.

Brijen Thananjeyan, Ashwin Balakrishna, Suraj Nair, Michael Luo, Krishnan Srinivasan, Minho Hwang, Joseph E. Gonzalez, Julian Ibarz, Chelsea Finn, and Ken Goldberg. Recovery RL: safe reinforcement learning with learned recovery zones. *IEEE Robotics Autom. Lett.*, 6(3):4915–4922, 2021. doi: 10.1109/LRA.2021.3070252. URL <https://doi.org/10.1109/LRA.2021.3070252>.

Daniel Toyama, Philippe Hamel, Anita Gergely, Gheorghe Comanici, Amelia Glaese, Zafarali Ahmed, Tyler Jackson, Shibli Mourad, and Doina Precup. Androidenv: A reinforcement learning platform for android. *arXiv preprint arXiv: Arxiv-2105.13231*, 2021.

Sam Toyer, Rohin Shah, Andrew Critch, and Stuart Russell. The MAGICAL benchmark for robust imitation. In Hugo Larochelle, Marc’Aurelio Ranzato, Raia Hadsell, Maria-Florina Balcan, and Hsuan-Tien Lin (eds.), *Advances in Neural Information Processing Systems 33: Annual Conference on Neural Information Processing Systems 2020, NeurIPS 2020, December 6-12, 2020, virtual*, 2020. URL <https://proceedings.neurips.cc/paper/2020/hash/d464b5ac99e74462f321c06ccacc4bff-Abstract.html>.

Maria Tsimpoukelli, Jacob Menick, Serkan Cabi, S. M. Ali Eslami, Oriol Vinyals, and Felix Hill. Multimodal few-shot learning with frozen language models. In Marc’Aurelio Ranzato, Alina Beygelzimer, Yann N. Dauphin, Percy Liang, and Jennifer Wortman Vaughan (eds.), *Advances in Neural Information Processing Systems 34: Annual Conference on Neural Information Processing Systems 2021, NeurIPS 2021, December 6-14, 2021, virtual*, pp. 200–212, 2021. URL <https://proceedings.neurips.cc/paper/2021/hash/01b7575c38dac42f3cfb7d500438b875-Abstract.html>.

Oriol Vinyals, Igor Babuschkin, Junyoung Chung, Michael Mathieu, Max Jaderberg, Wojciech M Czarnecki, Andrew Dudzik, Aja Huang, Petko Georgiev, Richard Powell, et al. Alphastar: Mastering the real-time strategy game starcraft ii. *DeepMind blog*, 2, 2019.

Peng Wang, An Yang, Rui Men, Junyang Lin, Shuai Bai, Zhikang Li, Jianxin Ma, Chang Zhou, Jingren Zhou, and Hongxia Yang. Ofa: Unifying architectures, tasks, and modalities through a simple sequence-to-sequence learning framework. *arXiv preprint arXiv: Arxiv-2202.03052*, 2022a.

Su Wang, Ceslee Montgomery, Jordi Orbay, Vighnesh Birodkar, Aleksandra Faust, Izzeddin Gur, Natasha Jaques, Austin Waters, Jason Baldridge, and Peter Anderson. Less is more: Generating grounded navigation instructions from landmarks. *arXiv preprint arXiv: Arxiv-2111.12872*, 2021.

Thomas Wang, Adam Roberts, Daniel Hesslow, Teven Le Scao, Hyung Won Chung, Iz Beltagy, Julien Launay, and Colin Raffel. What language model architecture and pretraining objective work best for zero-shot generalization? *Icml*, 2022b. doi: 10.48550/arXiv.2204.05832.

Wenhui Wang, Hangbo Bao, Li Dong, Johan Bjorck, Zhiliang Peng, Qiang Liu, Kriti Aggarwal, Owais Khan Mohammed, Saksham Singhal, Subhajit Som, and Furu Wei. Image as a foreign language: Beit pretraining for all vision and vision-language tasks. *arXiv preprint arXiv: Arxiv-2208.10442*, 2022c.

Jason Wei, Yi Tay, Rishi Bommasani, Colin Raffel, Barret Zoph, Sebastian Borgeaud, Dani Yogatama, Maarten Bosma, Denny Zhou, Donald Metzler, Ed H. Chi, Tatsunori Hashimoto, Oriol Vinyals, Percy Liang, Jeff Dean, and William Fedus. Emergent abilities of large language models. *arXiv preprint arXiv: Arxiv-2206.07682*, 2022.

Luca Weihs, Matt Deitke, Aniruddha Kembhavi, and Roozbeh Mottaghi. Visual room rearrangement. In *IEEE Conference on Computer Vision and Pattern Recognition, CVPR 2021, virtual, June 19-25, 2021*, pp. 5922–5931. Computer Vision Foundation / IEEE, 2021. doi: 10.1109/CVPR46437.2021.00586. URL https://openaccess.thecvf.com/content/CVPR2021/html/Weihs_Visual_Room_Rearrangement_CVPR_2021_paper.html.

Andrea Weikert, Andy Goralczyk, Basse Salmela, Ben Dansie, Campbell Barton, Enrico Valenza, Gleb Alexandrov, Ian Hubert, Kjartan Tysdal, Lech Sokolowski, Manu Järvinen, Massimiliana Pulieso, Matt Ebb, Pablo Vazquez, Rob Tuytel, Roland Hess, Sarah Feldlaufer, Sebastian König, Sebastian Platen, and Sönke Mäter. Blender online libraries for textures, 2022. URL <https://cloud.blender.org/p/textures/>.

Thomas Wolf, Lysandre Debut, Victor Sanh, Julien Chaumond, Clement Delangue, Anthony Moi, Pierrick Cistac, Tim Rault, Rémi Louf, Morgan Funtowicz, Joe Davison, Sam Shleifer, Patrick von Platen, Clara Ma, Yacine Jernite, Julien Plu, Canwen Xu, Teven Le Scao, Sylvain Gugger, Mariama Drame, Quentin Lhoest, and Alexander M. Rush. Huggingface’s transformers: State-of-the-art natural language processing. *arXiv preprint arXiv: Arxiv-1910.03771*, 2019.

Yuxin Wu, Alexander Kirillov, Francisco Massa, Wan-Yen Lo, and Ross Girshick. Detectron2. <https://github.com/facebookresearch/detectron2>, 2019.

Tete Xiao, Ilija Radosavovic, Trevor Darrell, and Jitendra Malik. Masked visual pre-training for motor control. *arXiv preprint arXiv:2203.06173*, 2022.

Mengdi Xu, Yikang Shen, Shun Zhang, Yuchen Lu, Ding Zhao, Joshua B. Tenenbaum, and Chuang Gan. Prompting decision transformer for few-shot policy generalization. *arXiv preprint arXiv: Arxiv-2206.13499*, 2022.

Ziyi Yang, Yuwei Fang, Chenguang Zhu, Reid Pryzant, Dongdong Chen, Yu Shi, Yichong Xu, Yao Qian, Mei Gao, Yi-Ling Chen, Liyang Lu, Yujia Xie, Robert Gmyr, Noel Codella, Naoyuki Kanda, Bin Xiao, Lu Yuan, Takuya Yoshioka, Michael Zeng, and Xuedong Huang. i-code: An integrative and composable multimodal learning framework. *arXiv preprint arXiv: Arxiv-2205.01818*, 2022.

Tianhe Yu, Deirdre Quillen, Zhanpeng He, Ryan Julian, Avnish Narayan, Hayden Shively, Adithya Bellathur, Karol Hausman, Chelsea Finn, and Sergey Levine. Meta-world: A benchmark and evaluation for multi-task and meta reinforcement learning. *arXiv preprint arXiv: Arxiv-1910.10897*, 2019.

Lu Yuan, Dongdong Chen, Yi-Ling Chen, Noel Codella, Xiyang Dai, Jianfeng Gao, Houdong Hu, Xuedong Huang, Boxin Li, Chunyuan Li, Ce Liu, Mengchen Liu, Zicheng Liu, Yumao Lu, Yu Shi, Lijuan Wang, Jianfeng Wang, Bin Xiao, Zhen Xiao, Jianwei Yang, Michael Zeng, Luwei Zhou, and Pengchuan Zhang. Florence: A new foundation model for computer vision. *arXiv preprint arXiv: Arxiv-2111.11432*, 2021.

Rowan Zellers, Ximing Lu, Jack Hessel, Youngjae Yu, Jae Sung Park, Jize Cao, Ali Farhadi, and Yejin Choi. Merlot: Multimodal neural script knowledge models. *arXiv preprint arXiv: Arxiv-2106.02636*, 2021.

Rowan Zellers, Jiasen Lu, Ximing Lu, Youngjae Yu, Yanpeng Zhao, Mohammadreza Salehi, Aditya Kusupati, Jack Hessel, Ali Farhadi, and Yejin Choi. Merlot reserve: Neural script knowledge through vision and language and sound. *CVPR*, 2022.

Andy Zeng, Pete Florence, Jonathan Tompson, Stefan Welker, Jonathan Chien, Maria Attarian, Travis Armstrong, Ivan Krasin, Dan Duong, Ayzaan Wahid, Vikas Sindhwani, and Johnny Lee. Transporter networks: Rearranging the visual world for robotic manipulation. *arXiv preprint arXiv: Arxiv-2010.14406*, 2020.

Andy Zeng, Adrian Wong, Stefan Welker, Krzysztof Choromanski, Federico Tombari, Aveek Purohit, Michael Ryoo, Vikas Sindhwani, Johnny Lee, Vincent Vanhoucke, and Pete Florence. Socratic models: Composing zero-shot multimodal reasoning with language. *arXiv preprint arXiv: Arxiv-2204.00598*, 2022.

Mandi Zhao, Fangchen Liu, Kimin Lee, and Pieter Abbeel. Towards more generalizable one-shot visual imitation learning. In *2022 International Conference on Robotics and Automation, ICRA 2022, Philadelphia, PA, USA, May 23-27, 2022*, pp. 2434–2444. IEEE, 2022. doi: 10.1109/ICRA46639.2022.9812450. URL <https://doi.org/10.1109/ICRA46639.2022.9812450>.

Qinqing Zheng, Amy Zhang, and Aditya Grover. Online decision transformer. *arXiv preprint arXiv: Arxiv-2202.05607*, 2022.

Yuke Zhu, Josiah Wong, Ajay Mandlekar, and Roberto Martín-Martín. robosuite: A modular simulation framework and benchmark for robot learning. *arXiv preprint arXiv: Arxiv-2009.12293*, 2020.

A SIMULATOR DETAILS

We build our VIMA-BENCH simulation suite upon the Ravens physics simulator (Zeng et al., 2020; Shridhar et al., 2021). Specifically, it is supported by PyBullet (Coumans & Bai, 2016–2021) with a Universal Robot UR5 arm. The size of the tabletop workspace is $0.5 \times 1\text{m}$. Our benchmark contains extensible sets of object geometries and textures. Instantiated from an object-texture combination, all object instances can be rendered as RGB images appeared in multimodal prompts. Figure A.1 displays all object geometries. Figure A.2 displays all textures.

The observation space of VIMA-BENCH includes RGB images from both frontal and top-down views. It also includes a one-hot vector $\in \{0, 1\}^2$ to indicate type of the end-effector $\in \{\text{suction cup, spatula}\}$. While a suction cup is equipped in most manipulation tasks, a spatula is used in particular for visual constraint tasks, where an agent is asked to “wipe” objects. VIMA-BENCH inherits the same action space from Zeng et al. (2020) and Shridhar et al. (2021), which consists of primitive actions of “pick and place” for tasks with a suction cup as the end effector, or “push” for tasks with a spatula. Both primitive actions contain two poses $\in \text{SE}(2)$ specifying target poses of the end effector. For the “pick and place” primitive, they represent the pick pose and the place pose. For the “push” primitive, they represent the push starting pose and push ending pose.

Similar to prior work (Zeng et al., 2020; Shridhar et al., 2021), VIMA-BENCH provides scripted oracles to generate successful demonstrations for all tasks. We leverage them to construct an offline imitation dataset for behavioral cloning. Given a prompt, these pre-programmed bots can access privileged information such as the correct object to pick and target location to place.

B TASK SUITE

We develop 17 meta tasks that belong to 6 diverse categories. Thousands of individual tasks and their corresponding multimodal prompts can be procedurally generated from these meta-task templates. We use PyBullet (Coumans & Bai, 2016–2021) as our backend and the default renderer to produce the RGB frames for training data and interactive test environments. For demonstration purpose, we apply the NVISII (Morrical et al., 2020) raytracing renderer to enhance the visual quality. We elaborate each meta task in the following subsections.

B.1 SIMPLE OBJECT MANIPULATION

This task category asks agents to follow basic instructions specified by multimodal prompts.

Task 01: Pick the specified object(s) and place it into the specified object.

- **Prompt:** Put the $\{\text{object}\}_1$ into the $\{\text{object}\}_2$.
- **Description:** The image placeholder $\{\text{object}\}_1$ is the object to be picked and the $\{\text{object}\}_2$ is the container object. The agent requires to recognize the objects with the correct color-shape combinations. To extend the difficulties, it supports more than one object to be picked or placed. For example, the prompt Put the $\{\text{object}\}_1$ and $\{\text{object}\}_2$ into the $\{\text{object}\}_3$. asks to pick two different objects and place into a target container. We uniformly sample different color-shape combos for objects to be picked and containers.
- **Success Criteria:** All specified object(s) to pick are within the bounds of the container object(s), with specified shapes and textures provided in the prompt.
- **Oracle Trajectory:** Shown in Fig. A.3 with its multimodal prompt.

Task 02: In the workspace, put the objects with a specified texture shown in the scene image in the prompt into container object(s) with a specified color. This task requires the agent to find the correct object to manipulate by grounding the textural attributes from both natural language descriptions and the visual scene images.

- **Prompt:** Put the $\{\text{texture}\}_1$ object in $\{\text{scene}\}$ into the $\{\text{texture}\}_2$ object .

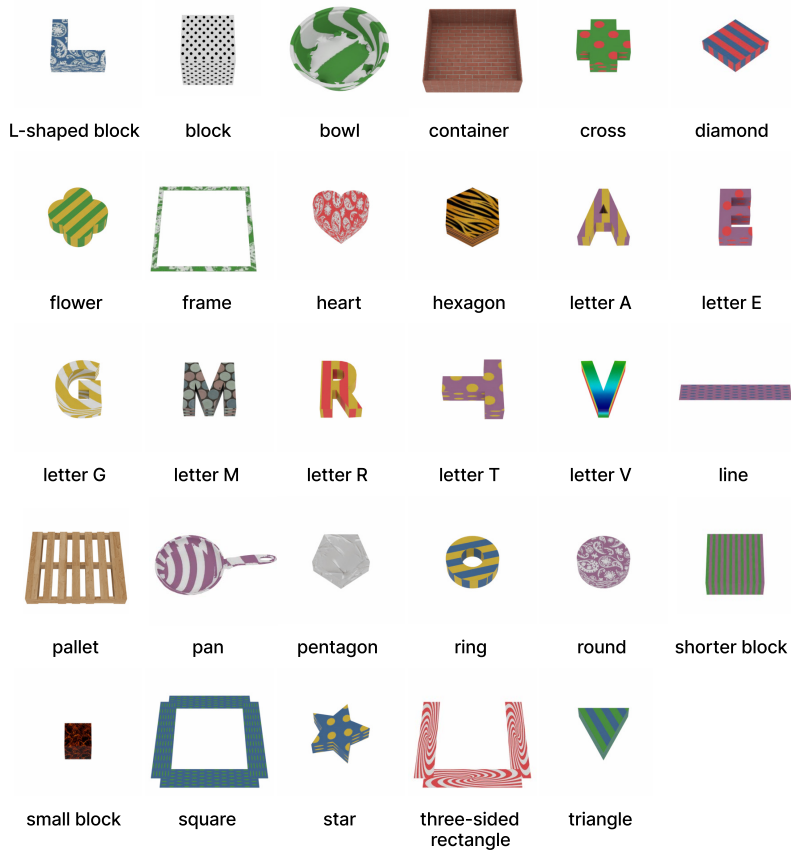


Figure A.1: **Object Gallery in VIMA-BENCH** textured with random textures. Bowl and pan are from Google Scanned Objects ([Downs et al., 2022](#)) while others are from Ravens ([Zeng et al., 2020](#))

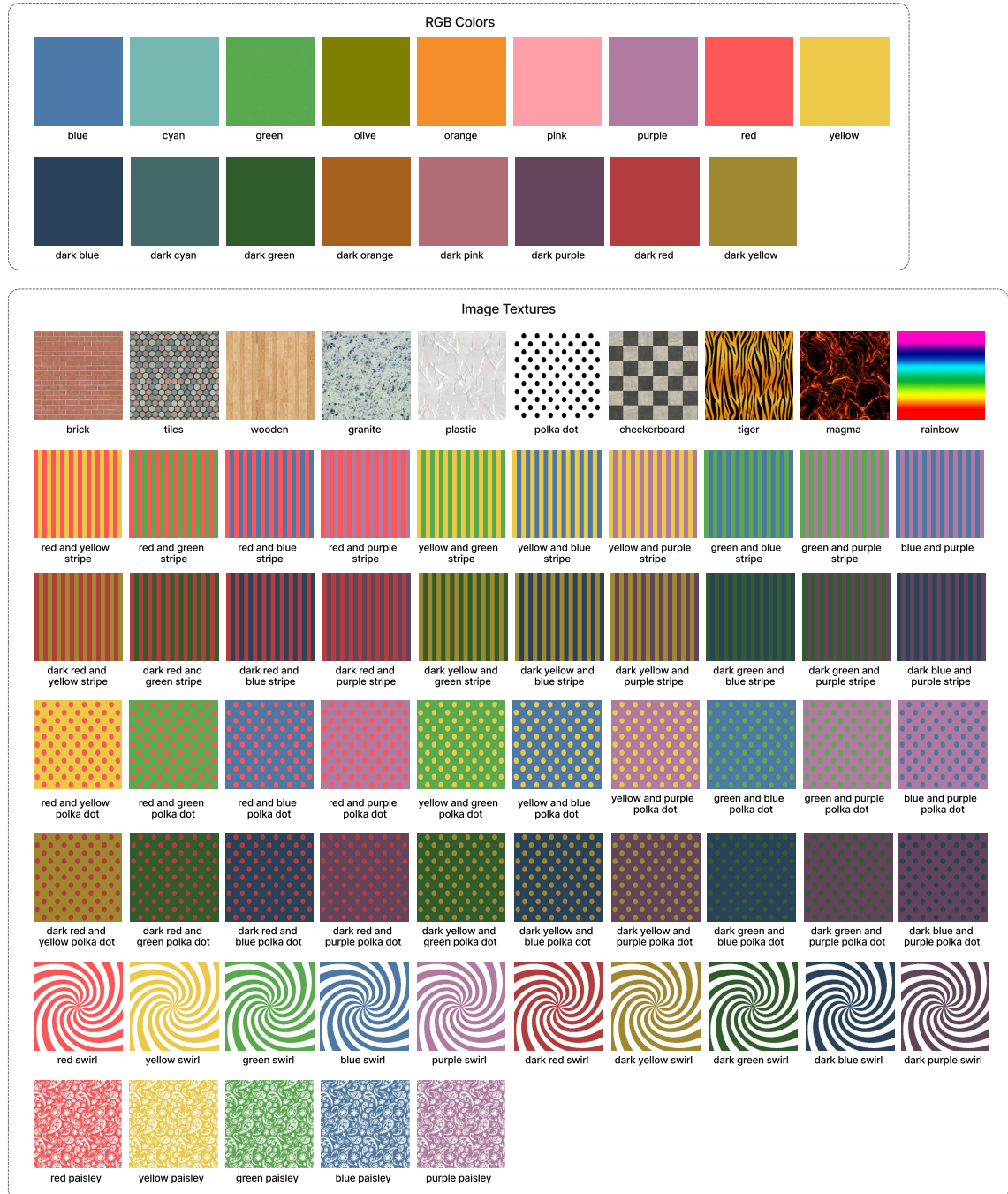


Figure A.2: **Texture Gallery in VIMA-BENCH**. The first row of image-based textures are from Blender Cloud Libraries (Weikert et al., 2022), while others are generated by ourselves.

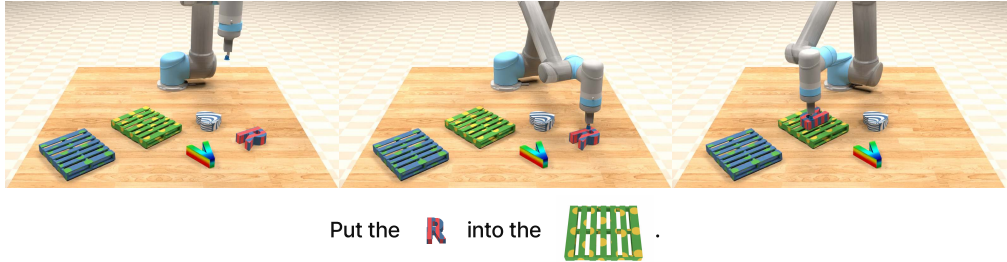


Figure A.3: Simple Object Manipulation: Task 01

- **Description:** The text placeholder $\{\text{texture}\}_1$ and $\{\text{texture}\}_2$ are sampled textures for objects to be picked and the container objects, respectively. The number of dragged objects with the same texture can be varied. $\{\text{scene}\}$ is the workspace-like image placeholder. There is a designated number of distractors with different textures (and potentially different shapes) in the scene. For each distractor in the workspace, it has 50% chance to be either dragged or container distractor object with different textures from those specified in the prompt.
- **Success Criteria:** All objects in the workspace with $\{\text{texture}\}_1$ are within the bounds of the container object with $\{\text{texture}\}_2$.
- **Oracle Trajectory:** Shown in Fig. A.4 with its multimodal prompt.



Figure A.4: Simple Object Manipulation: Task 02

Task 03: Rotate objects clockwise by certain degrees along z -axis. Only rotationally asymmetric objects are considered in this task.

- **Prompt:** Rotate the $\{\text{object}\}_1 \{\text{angles}\}$ degrees.
- **Description:** The agent is required to rotate all objects in the workspace specified by the image placeholder $\{\text{object}\}_1$. There are also objects with different color-shape combinations in the workspace as distractors. $\{\text{angles}\}$ is the sampled degree that the dragged object needs to be rotated. A target angle is sampled from 30° , 60° , 90° , 120° , and 150° .
- **Success Criteria:** The position of the specified object matches its original position, and the orientation matches the orientation after rotating specific angles.
- **Oracle Trajectory:** Shown in Fig. A.5 with its multimodal prompt.

B.2 VISUAL GOAL REACHING

This task category requires agents to manipulate objects in the workspace to reach goal states represented as images shown in prompts.



Rotate the 120 degrees.

Figure A.5: Simple Object Manipulation: Task 03

Task 04: Rearrange target objects in the workspace to match goal configuration shown in prompts. Note that to achieve the goal configuration, distractors may need to be moved away first.

- **Prompt:** Rearrange to this {scene}.
- **Description:** Objects in the scene placeholder {scene} are target objects to be manipulated and rearranged. In the workspace, the same target objects are spawned randomly, potentially with distractors randomly spawned as well. With a defined distractor conflict rate, the position of each distractor has this probability to occupy the position of any target object such that the rearrangement can only succeed if moving away that distractor first.
- **Success Criteria:** The configuration of target objects in the workspace matches that specified in the prompt.
- **Oracle Trajectory:** Shown in Fig. A.6 with its multimodal prompt. .

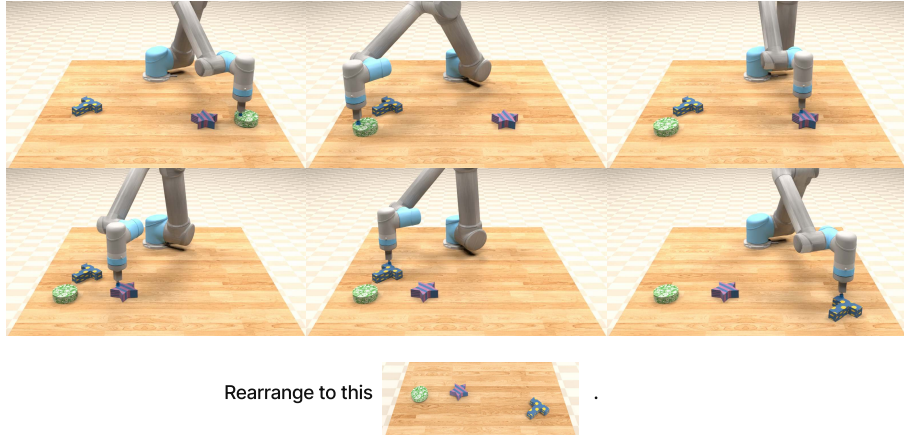


Figure A.6: Visual Goal Reaching: Task 04

Task 05: Extend the task 04 by requiring the agent to restore rearranged objects to the initial setup after the “rearranging” phase.

- **Prompt:** Rearrange objects to this setup {scene} and then restore.
- **Description:** Same as the task 04, except introducing the instruction “restore”.
- **Success Criteria:** Meet the success criteria of the task 04, and then within the allowed max steps restore all target objects to their initial configurations.
- **Oracle Trajectory:** Shown in Fig. A.7 with its multimodal prompt.

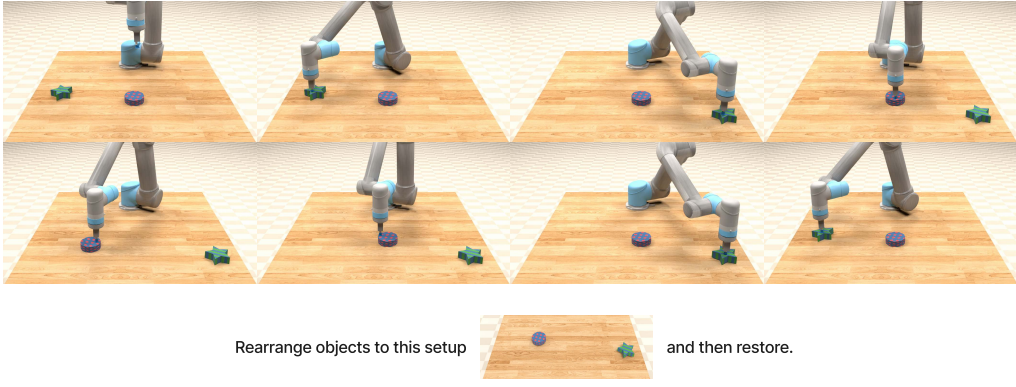


Figure A.7: Visual Goal Reaching: Task 05

B.3 NOVEL CONCEPT GROUNDING

This task category requires agents to ground new concepts of adjectives, nouns, or verbs via visual perception and language understanding. Prompts consist of two parts: a definition part followed by an instruction part. In the definition part, novel conceptions are defined by multimodal illustrations with multiple support examples. In the instruction part, agents are asked to achieve the goal by properly applying concepts from the definition part. The assignment of unique nonsense words is varied and independent for each task instance such that tasks can only be solved if the agent applies the reasoning correctly. This ability is also referred to as *fast-mapping* (Heibeck & Markman, 1987).

Task 06: Ground comparative adjectives by comparing the size or the textural saturation of objects and manipulating the correct object(s) instructed in the prompt.

- **Prompt:** $\{\text{demo_object}\}_1$ is $\{\text{novel_adj}\}$ than $\{\text{demo_object}\}_2$. Put the $\{\text{adv}\} \{\text{novel_adj}\} \{\text{object}\}_1$ into the $\{\text{object}\}_2$.
- **Description:** The sampled adjective $\{\text{novel_adj}\}$ is a dummy adjective placeholder for agent to ground. By default, the novel adjective set is $\{\text{daxer, blicker, modier, kobar}\}$. The real meaning can be related to size (smaller/larger) or textural saturation (lighter/darker texture). The image placeholders $\{\text{demo_object}\}_1$ and $\{\text{demo_object}\}_2$ illustrate how the novel adjective is defined. For example, if the real comparison is "taller", then the sampled object in $\{\text{demo_object}\}_1$ is taller than $\{\text{demo_object}\}_2$. The choices of the novel adjective and the real meaning are independently sampled for different task instances. For the instruction part, this task is similar to task 01, where the agent is required to pick the specified dragged object(s) with the novel adjective attribute and then place it into the specified container object. To avoid revealing the correct object to manipulate, we use a neutral texture for objects appeared in the instruction part.
- **Success Criteria:** All target objects with the specified adjective attribute are within the bounds of the specified container object.
- **Oracle Trajectory:** Shown in Fig. A.8 with its multimodal prompt.

Task 07: Orthogonal to task 06 by requiring to learn mappings of novel nouns.

- **Prompt:** This is a $\{\text{novel_name}\}_1 \{\text{object}\}_1$. This is a $\{\text{novel_name}\}_2 \{\text{object}\}_2$. Put $\{\text{novel_name}\}_1$ into a $\{\text{novel_name}\}_2$.
- **Description:** Novel noun words are defined with the text placeholders $\{\text{novel_name}\}_1$ and $\{\text{novel_name}\}_2$, following their image placeholders $\{\text{object}\}_1$ and $\{\text{object}\}_2$, for the target object and container object, respectively. Novel nouns are sampled from $\{\text{dax, blicket, wug, zup}\}$. In the instruction part, objects are expressed as novel nouns defined in the previous definition part. Distractors are defined the same as task 01.



Figure A.8: Novel Concept Grounding: Task 06

- **Success Criteria:** All target object(s) are within the bounds of the container object(s).
- **Oracle Trajectory:** Shown in Fig. A.8 with its multimodal prompt.

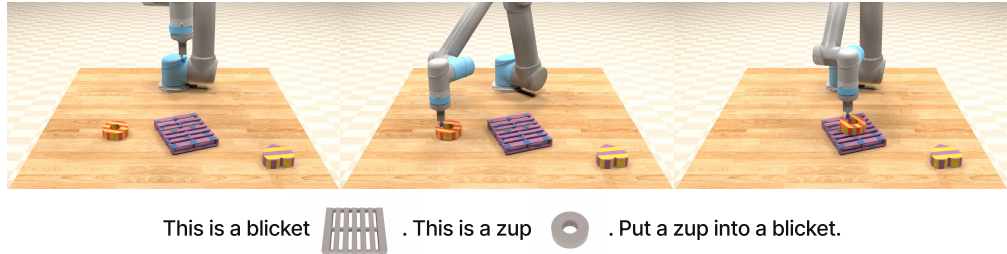


Figure A.9: Novel Concept Grounding: Task 07

Task 08: Combination of tasks 06 and 07.

- **Prompt:** This is a {novel_name}₁ {object}₁. This is a {novel_name}₂ {object}₂. {demo_object}₁ is {adj} than {demo_object}₂. Put the {adv} {novel_adj} {novel_name}₁ into the {novel_name}₂.
- **Description:** see task description for task 06 and task 07.
- **Success Criteria:** Similar as tasks 06 and 07.
- **Oracle Trajectory:** Shown in Fig. A.10 with its multimodal prompt.

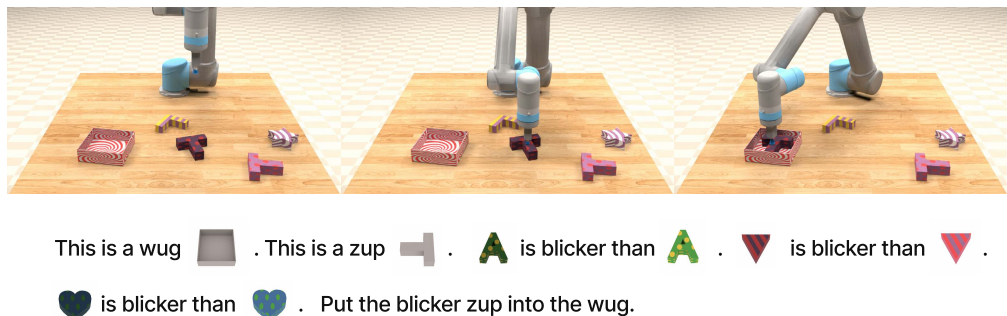


Figure A.10: Novel Concept Grounding: Task 08

Task 09: A novel verb "twist" is defined as rotating a specific angle conveyed by several examples. This task is similar to task 03, but it requires the agent to infer what is the exact angle to rotate from the prompt and to ground novel verbs that are semantically similar but different in exact definitions.

- **Prompt:** "Twist" is defined as rotating object a specific angle. For examples: From $\{\text{before_twist}\}_i$ to $\{\text{after_twist}\}_i$. Now twist all $\{\text{texture}\}$ objects.
- **Description:** Both $\{\text{before_twist}\}_i$ and $\{\text{after_twist}\}_i$ are scene placeholders where $\{\text{before_twist}\}_i$ shows a randomly sampled object before "twist" and $\{\text{after_twist}\}_i$ shows the same object pose after "twist". All examples illustrate the same sampled angle of the rotation. In the workspace, the target objects have the texture specified by $\{\text{texture}\}$ and randomly sampled shapes.
- **Success Criteria:** Same as the task 03.
- **Oracle Trajectory:** Shown in Fig. A.11 with its multimodal prompt.



"Twist" is defined as rotating object a specific angle. For examples:



Figure A.11: Novel Concept Grounding: Task 09

B.4 ONE-SHOT VIDEO IMITATION

This task category requires agents to imitate motions demonstrated through videos shown in prompts.

Task 10: Follow motions for specific objects.

- **Prompt:** Follow this motion for $\{\text{object}\}$: $\{\text{frame}\}_1 \dots \{\text{frame}\}_i \dots \{\text{frame}\}_n$.
- **Description:** Image placeholder $\{\text{object}\}$ is the target object to be manipulated and $\{\{\text{frame}\}_i\}$ is set of workspace-like scene placeholders to represent a video trajectory, where n is the trajectory length. There is an object spawned at the center in both the workspace and the prompt video but with different textures as a distractor. The initial position of the target object matches that in $\{\text{frame}\}_1$.
- **Success Criteria:** In each step, the pose of the target object matches the pose in the corresponding video frame. Incorrect manipulation sequences are considered as failures.
- **Oracle Trajectory:** Shown in Fig. A.12 with its multimodal prompt.

Task 11: Stack objects with the order illustrated in the prompt video.

- **Prompt:** Stack objects in this order $\{\text{frame}\}_1 \dots \{\text{frame}\}_i \dots \{\text{frame}\}_n$.
- **Description:** There are multiple objects with the same shape but different textures spawned in the workspace without any stacking initially. Distractor objects with different shapes are spawned in the workspace but not in the prompt video. At each step of the prompt video, one of the top objects is stacked over another object or put at an empty position.

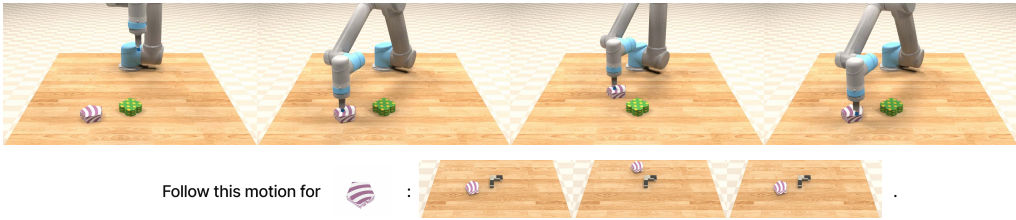


Figure A.12: One-shot video imitation: Task 10

- **Success Criteria:** Similar as task 10.
- **Oracle Trajectory:** Shown in Fig. A.13 with its multimodal prompt.

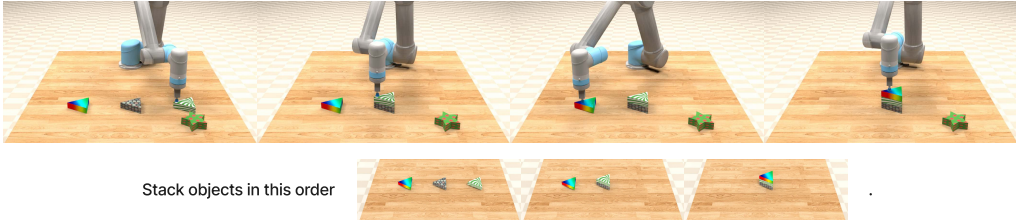


Figure A.13: One-shot video imitation: Task 11

B.5 VISUAL CONSTRAINT SATISFACTION

This task category requires agents to wipe a specific number of objects in the workspace to a goal region while also satisfy the given visual constraint.

Task 12: Sweep the designated number of objects into a specified region without exceeding the boundary.

- **Prompt:** Sweep {quantifier} {object} into {bounds} without exceeding {constraint}.
- **Description:** {object} is the image placeholder of the target object to be swept spawned with a random amount in the workspace. Distractors have the same amount, same shape, but different color from target objects. {quantifier} is the text placeholder to determine the target quantity of objects to be wiped, sampled from any, one, two, three, and all. {bounds} is the image placeholder for a three-sided rectangle as the goal region. {constraint} is the constraint line.
- **Success Criteria:** The exact number of target objects to be swept are all inside the specified region. Failure reasons include 1) any distractor being wiped into the region, 2) target object exceeding the constraint, or 3) incorrect number of target objects being swept into the goal region.
- **Oracle Trajectory:** Shown in Fig. A.14 with its multimodal prompt.

Task 13: Sweep the designated number of objects into a specified region without touching the constraint.

- **Prompt:** Sweep {quantifier} {object} into {bounds} without touching {constraint}.
- **Description:** Similar as task 12 but requiring different way to satisfy the constraint. The agent has to learn to avoid "touching" the constraint line in this case.



Figure A.14: Visual Constraint Satisfaction: Task 12

- **Success Criteria:** Similar as task 12 except that the constraint is to not touch the red line.
- **Oracle Trajectory:** Shown in Fig. A.15 with its multimodal prompt.

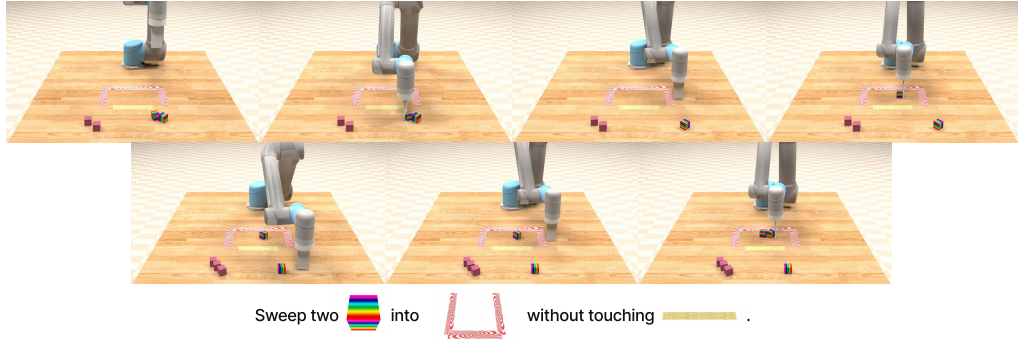


Figure A.15: Visual Constraint Satisfaction: Task 13

B.6 VISUAL REASONING

This task category requires agents to make decisions by reasoning over or memorizing information conveyed through multimodal prompts.

Task 14: By reasoning the "same texture", the agent is required to pick all objects in the workspace with the same texture as the container objects specified in the prompt and place them into it.

- **Prompt:** Put all objects with the same texture as {object} into it.
- **Description:** {object} is the sampled goal container object. In the workspace, there are objects with the same texture as the container but potentially different shapes. Distractors with different textures are spawned.
- **Success Criteria:** All objects with the same texture as the goal container are within the bounds of the container.
- **Oracle Trajectory:** Shown in Fig. A.16 with its multimodal prompt.

Task 15: By reasoning the "same shape", the agent is required to pick all objects in the workspace with the same top-down shape as the goal container specified in the prompt and place them into it. For example, blocks and boxes have the same rectangular shape.

- **Prompt:** Put all objects with the same profile as {object} into it.

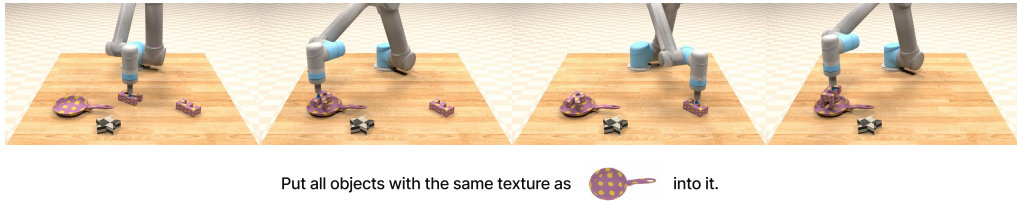


Figure A.16: Visual Reasoning: Task 14

- **Description:** Similar to the task 14 except the objects to be picked and placed are with the same shape. There are three different shapes: *rectangular-like* (e.g. block and pallet), *circle-like* (e.g. ring and bowl), and *undetermined* for the rest.
- **Success Criteria:** All objects with the same shape as the container are within the container.
- **Oracle Trajectory:** Shown in Fig. A.17 with its multimodal prompt.

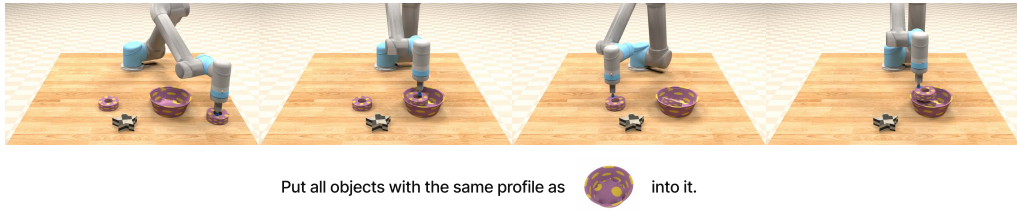


Figure A.17: Visual Reasoning: Task 15

Task 16: Put the target object into the container, and then put one of its old neighbors into the same container.

- **Prompt:** First put $\{\text{object}\}_1$ into $\{\text{object}\}_2$ then put the object that was previously at its $\{\text{direction}\}$ into the same $\{\text{object}\}_2$.
- **Description:** Objects in image placeholders $\{\text{object}\}_1$ and $\{\text{object}\}_2$ are the target object to be picked and the container, respectively. We then ask the agent to put one of old neighbors of the previous target object into the same container. The old neighboring object is specified through cardinal directions {north, south, west, east}.
- **Success Criteria:** The target object and the correct neighboring object are inside the container.
- **Oracle Trajectory:** Shown in Fig. A.18 with its multimodal prompt.

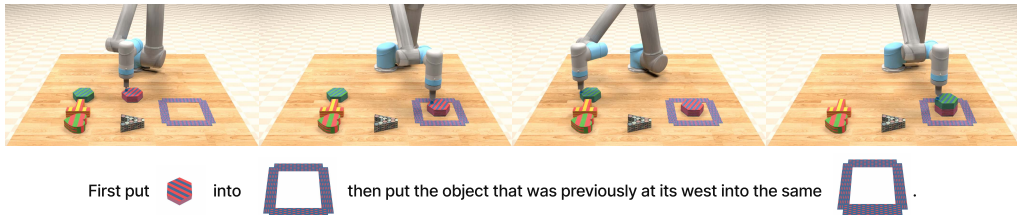


Figure A.18: Visual Reasoning: Task 16

Task 17: Pick and place the target object specified in the prompt into different containers in order then restore to the initial container.

- **Prompt:** Put $\{\text{object}\}_1$ into $\{\text{object}\}_2$. Finally restore it into its original container.
- **Description:** The object in the image placeholder $\{\text{object}\}_1$ is the target object to be manipulated across the task. There are more than one target containers (e.g. Put $\{\text{object}\}_1$ into $\{\text{object}\}_2$ then $\{\text{object}\}_3$. Finally restore it into its original container. for two target base objects to be placed in order). The rest of spawned containers naturally becomes distractors.
- **Success Criteria:** The target object are first put into multiple containers following the specific order. Finally it should be restored into its original container.
- **Oracle Trajectory:** Shown in Fig.A.19 with its multimodal prompt.

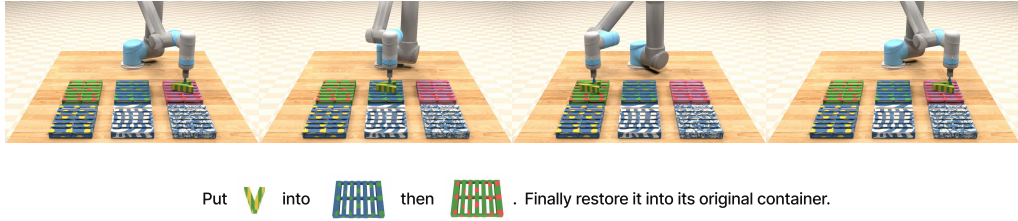


Figure A.19: Visual Reasoning: Task 17

C MODEL ARCHITECTURE

In this section, we provide comprehensive details about VIMA model architecture as well as other adapted baseline methods. We implement all models in PyTorch (Paszke et al., 2019) and adapt Transformer-related implementation from Wolf et al. (2019).

C.1 VIMA ARCHITECTURE

C.1.1 MULTIMODAL PROMPT TOKENIZATIONS

As introduced in Section 4, there are 3 types of input formats in multimodal prompts, namely (1) **text inputs**, (2) **images of full scenes**, and (3) **images of single objects**.

For **text inputs**, we follow the standard pipeline in NLP to first tokenize raw languages to discrete indices through pre-trained t5-base tokenizer. We then obtain corresponding word tokens from the embedding look-up of the pre-trained t5-base model. For **images of full scenes**, we first parse the scene through a fine-tuned mask R-CNN detection model (He et al., 2017; Wu et al., 2019) to extract individual objects. Each object representation contains a bounding box and a cropped image. The bounding box is in the format of $[x_{\text{center}}, y_{\text{center}}, \text{height}, \text{width}]$. We normalize it to be within $[0, 1]$ by dividing each dimension with corresponding upper-bound value. We then pass it through a bounding box encoder MLP and obtain a feature vector. To process the cropped image, we first pad non-square image to a square by padding along the shorter dimension. We then resize it to a pre-configured size and pass it through a ViT (trained from scratch) to obtain the image feature. Finally, an object token is obtained by concatenating the bounding box feature and the image feature and mapping to the embedding dimension. For **images of single objects**, we obtain tokens in the same way except with a dummy bounding box. Detailed model hyperparameters about tokenizations are listed in Table 1.

After obtaining a sequence of prompt tokens, we follow Tsimpoukelli et al. (2021) to pass it through a pre-trained t5-base encoder to obtain encoded prompt. Note that we add adapter MLP between object tokens and the T5 encoder. We adopt learned absolute positional embedding. Model hyperparameters are listed in Table 1 as well.

Table 1: Model hyperparameters for multimodal prompt tokenization.

| Hyperparameter | Value |
|-------------------------|-------------------|
| Text Tokenization | |
| Tokenizer | t5-base tokenizer |
| Embedding Dimension | 768 |
| Image Tokenization | |
| ViT Input Image Size | 32 × 32 |
| ViT Patch Size | 16 |
| ViT Width | 768 |
| ViT Layer | 4 |
| ViT Number of Heads | 24 |
| Bounding Box MLP | |
| Hidden Dimension | 768 |
| Hidden Depth | 2 |
| Prompt Encoding | |
| Pre-trained LM | t5-base |
| Unfreeze Last N Layers | 2 |
| Positional Embedding | Absolute |
| Token Adapter MLP Depth | 2 |

C.1.2 OBSERVATION ENCODING

Since all RGB observations are images of full scenes, we follow the same procedure discussed above to obtain flattened object tokens. Because we provide RGBs from two views (frontal and top-down), we order object tokens by following the order of [frontal, top-down]. We one-hot encode the state of the end effector. We then concatenate object tokens with the end-effector state and transform to observation tokens. We adopt learned absolute positional embedding. Detailed model hyperparameters about observation encoding is provided in Table 2.

Table 2: Model hyperparameters for observation encoding.

| Hyperparameter | Value |
|----------------------------------|----------|
| Observation Token Dimension | 768 |
| End Effector Embedding Dimension | 2 |
| Positional Embedding | Absolute |

C.1.3 ACTION ENCODING

Since our model is conditioned on observation-action interleaved history, we also tokenize past actions. We follow common practice in [Chen et al. \(2021\)](#); [Zheng et al. \(2022\)](#) to encode past actions with a two-layer MLP. It has a hidden dimension of 256. We then map outputs to token dimension and obtain action tokens.

C.1.4 SEQUENCE MODELING

The robot controller in VIMA is a causal decoder that autoregressively predicts actions. To condition the decoder on prompt tokens, we perform cross-attention between history tokens and prompt tokens (Figure 3). Concretely, we pass history tokens as the query sequence and prompt tokens as the key-value sequence into cross-attention blocks. The output prompt-aware trajectory tokens then go through causal self-attention blocks. We alternate cross-attention and self-attention L times. This procedure is technically described in Pseudocode 1.

```

def xattn_sequence_modeling(
    prompt_tokens,           # the [L, d] prompt tokens (L=prompt length)
    obs_tokens,              # the [T, d] obs tokens (T=time step)
    act_tokens,               # the [T-1, d] action tokens
    traj_pos_embd,           # learned positional embedding for trajectory
    prompt_pos_embd,          # learned positional embedding for prompt
):
    # interleave obs and action tokens
    traj_tokens = interleave(obs_tokens, act_tokens)  # [2T-1, d]
    # add positional embedding to trajectory tokens
    x = traj_tokens + traj_pos_embd
    # add positional embedding to prompt tokens
    prompt_tokens = prompt_tokens + prompt_pos_embd

    # apply xattn and causal self-attn
    for i in range(num_layers):
        # cross-attention
        x = x + attn_i(q=x, kv=prompt_tokens)
        # feed forward
        x = x + ffw_xattn_i(x)
        # self-attention
        x = x + causal_attn_i(q=x, kv=x)
        # feed forward
        x = x + ffw_i(x)

    # the last token is the predicted action token
    predicted_act_token = x[-1]
    return predicted_act_token

```

Pseudocode 1: Cross-attention operation that conditions the history on prompt. We repetitively alternate cross-attention and self-attention to model the trajectory given a specific task.

C.1.5 ACTION DECODING

After obtaining the predicted action token, we map it to the action space \mathcal{A} and obtain the predicted action. This is achieved through a group of action heads. Since the action space consists of two $\text{SE}(2)$ poses, for each pose we use six independent heads to decode discrete actions (two for xy coordinate and four for rotation represented in quaternion). These discrete actions are then de-discretized and mapped to continuous actions through affine transformation. The two poses are modeled independently. Early ablations show that this independent modeling is equally good as alternatives like autoregressive decoding (Vinyals et al., 2019; OpenAI et al., 2019). Detailed model hyperparameters are listed in Table 3.

Table 3: Model hyperparameters for action decoders.

| Hyperparameter | Value |
|------------------------|-------|
| Hidden Dimension | 512 |
| Hidden Depth | 2 |
| Activation | ReLU |
| X-axis Discrete Bins | 50 |
| Y-axis Discrete Bins | 100 |
| Rotation Discrete Bins | 50 |

C.2 BASELINES ARCHITECTURES

In this section, we elaborate model architectures for baseline methods. Some components such as the action decoder are same across all baseline methods and ours. Therefore, we only discuss unique model components.

Table 4: Model hyperparameters for ViT used in baseline methods.

| Hyperparameter | Value |
|----------------|----------|
| Image Size | 64 x 128 |
| Patch Size | 32 |
| ViT Width | 768 |
| ViT Layers | 4 |
| ViT Heads | 24 |

C.2.1 GATO

Gato (Reed et al., 2022) introduces a decoder-only model that solves tasks from multiple domains where tasks are specified by prompting the model with the observation and action subsequence. There are two differences between Gato and our method. (1) **Different visual tokenizers**. In Gato, observation tokens are represented as sequence of image patches instead of object tokens as in our method. In other words, Gato is not object-centric. (2) **Different prompt conditioning**. In Gato, prompt tokens are directly prepended to history tokens. This sequence of temporally concatenated tokens are then passed through a decoder-only model. In contrast, VIMA adopts cross-attention to condition the robot controller on the prompt (Fig. 3). Hyperparameters of Gato’s ViT is listed in Table 4. The decoder-style sequence modling is technically illustrated in Pseudocode 2.

```

def causal_sequence_modeling(
    prompt_tokens,      # the [L, d] prompt tokens (L=prompt length)
    sep_token,          # the [1, d] learned separator token
    obs_tokens,         # the [T, d] obs tokens (T=time step)
    act_tokens,         # the [T-1, d] action tokens
    pos_embd,          # learned positional embedding
):
    # interleave obs and action tokens
    traj_tokens = interleave(obs_tokens, act_tokens)    # [2T-1, d]
    # assemble input tokens
    x = concat([prompt_tokens, sep_token, traj_tokens])
    x = x + pos_embd

    # apply GPT layers with causal mask
    for i in range(num_layers):
        # self-attention
        x = x + causal_attn_i(q=x, kv=x)
        # feed forward
        x = x + ffw_i(x)

    # the last token is the predicted action token
    predicted_act_token = x[-1]
    return predicted_act_token

```

Pseudocode 2: Plain sequence modeling that temporally concatenates prompt and trajectory history and repetitively perform causal self-attention operation.

C.2.2 FLAMINGO

Flamingo (Alayrac et al., 2022) is a vision-language model that learns to generate textual completion in response to multimodal prompts. It embeds a variable number of prompt images into a fixed number of tokens via the *Perceiver Resampler* module (Jaegle et al., 2021b), and conditions the language decoder on the encoded prompt by cross-attention. Because the original Flamingo does not support embodied agents altogether, we have made major changes to adapt the architecture to robot learning. First, we swap the LLM component of Flamingo with our robot controller, which is a transformer decoder that outputs robot arm actions at every environment step (hyperparameters listed in Table 3). Second, VIMA uses an object-centric tokenizer instead of *Perceiver Resampler* that operates directly on raw RGB. We refer interested readers to Section 3.1 in Alayrac et al. (2022)

for a more detailed technical discussion on Flamingo’s architecture design. Model hyperparameters for our reimplementation of the *Perceiver Resampler* is listed in Table 5.

Table 5: Model hyperparameters for Perceiver Resampler used in Flamingo method.

| Hyperparameter | Value |
|--------------------------|-------|
| Number of Latent Queries | 4 |
| Number of Blocks | 4 |
| Self-attn per Block | 4 |
| Self-attn Heads | 24 |
| Cross-attn Heads | 24 |

C.2.3 DECISION TRANSFORMER

Decision Transformer (DT) (Chen et al., 2021; Janner et al., 2021) is among the first works to reinterpret the RL problem as transformer sequence modeling. In visual RL domains like Atari games, DT is prompted on the desired reward value and outputs actions autoregressively given the RGB observation embedding. We replace DT’s initial reward prompt with our multimodal task prompt embeddings, and remove all subsequent reward tokens. For visual tokenizer, we employ a learned ViT with hyperparameters listed in Table 4 to map an observed image to a single “state” token.

C.3 MASK R-CNN DETECTION MODEL

Finally, we elaborate the mask R-CNN model (He et al., 2017) for scene parsing and object extraction. We fine-tuned a pre-trained lightweight mask R-CNN (mask_rcnn_R_50_FPN_3x) from Wu et al. (2019) to adapt to scenes and images in our tabletop environment. A visualization of its output is provided in Figure A.20. We do not use the predicted object names in our models.

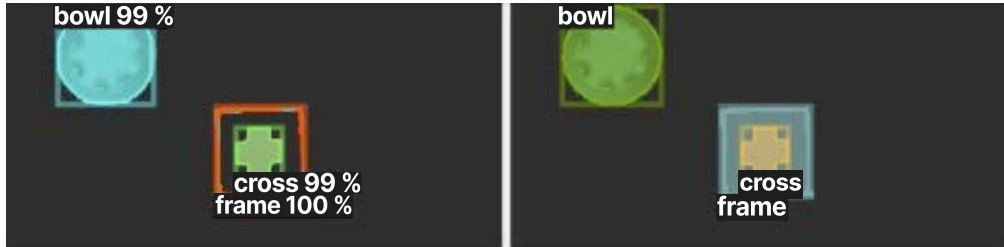


Figure A.20: Visualization of fine-tuned mask R-CNN. Left: Prediction from the detection model. Right: Ground-truth scene parsing. The detection model agrees well with ground-truth objects.

D VIMA TRAINING DETAILS

We follow the best practices to train Transformer models using the AdamW optimizer (Loshchilov & Hutter, 2019), learning rate warm-up, cosine annealing (Loshchilov & Hutter, 2017), etc. Training hyperparameters are provided in Table 6. We use GEGLU activation (Shazeer, 2020) inside Transformer models across all methods.

To make trained models robust to detection inaccuracies and failures, we apply *object augmentation* by randomly injecting *false-positive* detection outputs. Concretely, for observation at each time step, we sample number of augmented objects i.i.d. $n_{\text{augmented objects}} \sim \text{Cat}(K, \mathbf{p})$, where $\text{Cat}(\cdot)$ denotes a multi-categorical distribution with K supports parameterized by \mathbf{p} . For each augmented object, we then randomly sample a bounding box and corresponding cropped image to add to object tokens. In our experiments, we set $\mathbf{p} = \{0 : 0.95, 1 : 0.05\}$ with $K = 2$.

Table 6: Hyperparameters used during training.

| Hyperparameter | Value |
|---------------------------|--------|
| Learning Rate | 0.0001 |
| Warmup Steps | 7K |
| LR Cosine Annealing Steps | 17K |
| Weight Decay | 0 |
| Dropout | 0.1 |
| Gradient Clip Threshold | 1.0 |

D.1 VARY MODEL CAPACITY

We train a spectrum of 7 models ranging from 2M to 200M parameters. To vary the model capacity, we follow prior work ([Chowdhery et al., 2022](#)) to change embedding dimension and number of layers. We list configurations for methods with cross-attention prompt conditioning (i.e., ours and Flamingo) in Table 7, and configurations for methods only with causal self-attention (i.e., Gato and DT) in Table 8.

Table 7: Configurations for different sized models with cross-attention prompt conditioning.

| Model Size (M) | Embedding Dimension | Num Blocks | X-attn Heads | Self-attn Heads |
|----------------|---------------------|------------|--------------|-----------------|
| 2 | 256 | 1 | 8 | 8 |
| 4 | 256 | 2 | 8 | 8 |
| 9 | 320 | 3 | 10 | 10 |
| 20 | 384 | 4 | 12 | 12 |
| 43 | 512 | 5 | 16 | 16 |
| 92 | 640 | 7 | 20 | 20 |
| 200 | 768 | 11 | 24 | 24 |

Table 8: Configurations for different sized models with causal self-attention prompt conditioning.

| Model Size (M) | Embedding Dimension | Num Blocks | Self-attn Heads |
|----------------|---------------------|------------|-----------------|
| 2 | 64 | 1 | 2 |
| 4 | 96 | 2 | 3 |
| 9 | 192 | 3 | 6 |
| 20 | 320 | 4 | 10 |
| 43 | 512 | 5 | 16 |
| 92 | 768 | 7 | 24 |
| 200 | 768 | 18 | 24 |

E MORE EXPERIMENT RESULTS

E.1 BREAKDOWN RESULTS

We show breakdown results for Figure 4 in Tables 9, 10, 11, and 12, respectively.

E.2 VARY T5 ENCODER SIZES

We vary the size of the pre-trained T5 encoder ([Raffel et al., 2020](#)) to study the effect of prompt encoding. We experiment with three T5 model capacities: t5-small (30M), t5-base (111M), to t5-large (368M). For all T5 variants, we fine-tune the last two layers and freeze all other layers. We fix the parameter count of the decision-making part to be 200M. As shown in Table 13, we find no significant difference among the variants. Thus we set the standard t5-base as default for all our models.

Table 9: L1 level generalization results. Model indicates robot controller parameter count.

| Model | Method | Task 01 | Task 02 | Task 03 | Task 04 | Task 05 | Task 06 | Task 07 | Task 09 | Task 11 | Task 12 | Task 15 | Task 16 | Task 17 |
|-------|----------|--------------|--------------|--------------|--------------|-------------|--------------|--------------|-------------|-------------|-------------|-------------|-------------|-------------|
| 2M | Ours | 100.0 | 100.0 | 100.0 | 96.0 | 37.0 | 100.0 | 100.0 | 9.5 | 87.0 | 64.0 | 93.5 | 45.0 | 63.0 |
| | Gato | 62.0 | 61.0 | 22.5 | 13.5 | 7.0 | 44.5 | 54.0 | 4.0 | 48.0 | 85.0 | 44.5 | 43.0 | 0.0 |
| | Flamingo | 56.0 | 56.0 | 53.5 | 36.5 | 37.5 | 45.0 | 55.5 | 3.5 | 54.0 | 83.5 | 40.5 | 28.5 | 2.0 |
| | DT | 59.5 | 50.5 | 7.5 | 7.0 | 0.5 | 43.5 | 49.5 | 2.0 | 61.5 | 76.5 | 27.5 | 5.0 | 0.0 |
| 20M | Ours | 100.0 | 100.0 | 100.0 | 99.5 | 59.5 | 100.0 | 100.0 | 13.5 | 74.0 | 72.5 | 96.5 | 39.5 | 47.5 |
| | Gato | 61.5 | 62.0 | 32.5 | 49.0 | 38.0 | 46.0 | 60.0 | 5.0 | 68.0 | 83.0 | 47.0 | 46.5 | 2.0 |
| | Flamingo | 63.0 | 61.5 | 55.0 | 50.0 | 42.5 | 41.5 | 58.0 | 6.0 | 62.0 | 83.0 | 44.0 | 38.5 | 1.0 |
| | DT | 60.5 | 64.0 | 50.5 | 44.0 | 41.0 | 48.0 | 61.5 | 7.0 | 85.0 | 84.0 | 44.5 | 39.0 | 2.5 |
| 200M | Ours | 100.0 | 100.0 | 99.5 | 100.0 | 56.5 | 100.0 | 100.0 | 18.0 | 77.0 | 93.0 | 97.0 | 76.5 | 43.0 |
| | Gato | 79.0 | 68.0 | 91.5 | 57.0 | 44.5 | 54.0 | 74.0 | 18.0 | 61.0 | 88.5 | 83.5 | 33.5 | 2.5 |
| | Flamingo | 56.0 | 58.5 | 63.0 | 48.5 | 38.0 | 48.5 | 62.5 | 3.5 | 66.5 | 86.0 | 40.0 | 43.5 | 2.5 |
| | DT | 62.0 | 57.5 | 41.0 | 55.5 | 45.5 | 47.5 | 54.5 | 8.5 | 77.0 | 81.5 | 41.0 | 38.0 | 0.5 |

Table 10: L2 level generalization results. Model indicates robot controller parameter count.

| Model | Method | Task 01 | Task 02 | Task 03 | Task 04 | Task 05 | Task 06 | Task 07 | Task 09 | Task 11 | Task 12 | Task 15 | Task 16 | Task 17 |
|-------|----------|--------------|--------------|--------------|--------------|-------------|--------------|--------------|-------------|-------------|-------------|-------------|-------------|-------------|
| 2M | Ours | 100.0 | 100.0 | 100.0 | 95.5 | 37.5 | 100.0 | 100.0 | 17.5 | 87.5 | 67.0 | 97.5 | 46.0 | 54.5 |
| | Gato | 49.5 | 49.0 | 23.0 | 17.5 | 0.5 | 47.5 | 46.5 | 5.5 | 50.0 | 82.5 | 49.0 | 42.0 | 0.5 |
| | Flamingo | 45.5 | 46.0 | 56.0 | 39.5 | 35.5 | 49.0 | 47.0 | 9.0 | 53.0 | 80.0 | 43.0 | 29.5 | 1.0 |
| | DT | 51.0 | 45.5 | 9.5 | 7.0 | 0.5 | 45.5 | 45.0 | 0.0 | 65.0 | 81.5 | 32.0 | 5.0 | 0.0 |
| 20M | Ours | 100.0 | 100.0 | 100.0 | 100.0 | 61.0 | 100.0 | 100.0 | 16.5 | 75.5 | 75.0 | 96.0 | 37.5 | 47.5 |
| | Gato | 44.0 | 51.5 | 39.0 | 51.0 | 38.5 | 47.5 | 52.5 | 6.0 | 65.5 | 84.0 | 52.5 | 40.5 | 1.0 |
| | Flamingo | 48.5 | 49.0 | 55.5 | 48.0 | 42.5 | 46.5 | 52.0 | 6.0 | 66.0 | 82.0 | 47.5 | 37.0 | 0.5 |
| | DT | 50.5 | 49.5 | 53.0 | 44.5 | 43.5 | 47.0 | 46.0 | 8.0 | 83.5 | 80.0 | 46.5 | 41.0 | 2.5 |
| 200M | Ours | 100.0 | 100.0 | 99.5 | 100.0 | 54.5 | 100.0 | 100.0 | 17.5 | 77.0 | 93.0 | 98.5 | 75.0 | 45.0 |
| | Gato | 56.5 | 53.5 | 88.0 | 55.5 | 43.5 | 55.5 | 53.0 | 14.0 | 63.0 | 90.5 | 81.5 | 33.0 | 4.0 |
| | Flamingo | 51.0 | 52.5 | 61.5 | 49.5 | 38.5 | 47.5 | 55.5 | 5.5 | 70.5 | 82.0 | 42.0 | 39.0 | 3.0 |
| | DT | 52.0 | 52.0 | 49.5 | 54.5 | 45.5 | 52.5 | 51.0 | 11.0 | 76.5 | 84.0 | 43.0 | 38.0 | 0.5 |

Table 11: L3 level generalization results. Model indicates robot controller parameter count.

| Model | Method | Task 01 | Task 02 | Task 03 | Task 04 | Task 05 | Task 06 | Task 07 | Task 09 | Task 11 | Task 15 | Task 16 | Task 17 |
|-------|----------|--------------|--------------|------------|-------------|-------------|--------------|-------------|-------------|-------------|-------------|-------------|-------------|
| 2M | Ours | 100.0 | 100.0 | 100 | 98.0 | 34.5 | 100.0 | 99.5 | 17.0 | 97.5 | 94.0 | 48.5 | 39.0 |
| | Gato | 45.5 | 48 | 28.0 | 23.0 | 3.0 | 45.5 | 45.0 | 2.5 | 40.5 | 29.5 | 37.0 | 1 |
| | Flamingo | 41.5 | 54.5 | 50.5 | 39.5 | 29 | 45.0 | 49.5 | 5.5 | 57.5 | 22.5 | 25.0 | 0.0 |
| | DT | 48.5 | 50.0 | 5.0 | 7.0 | 2.5 | 47 | 45.5 | 2.0 | 69.5 | 22.5 | 5.0 | 0.0 |
| 20M | Ours | 98.0 | 100.0 | 100 | 98.5 | 55.5 | 100.0 | 99.5 | 15.0 | 88.5 | 99.5 | 44.0 | 29.5 |
| | Gato | 46.5 | 55 | 44.5 | 57.0 | 31.5 | 47.5 | 51.5 | 2.5 | 72.5 | 30.5 | 44.0 | 0 |
| | Flamingo | 47.0 | 54.5 | 53.0 | 55.0 | 36 | 42.5 | 48.0 | 6.5 | 70.0 | 33.0 | 41.5 | 0.0 |
| | DT | 50.0 | 60.5 | 56.5 | 48.0 | 33.5 | 51 | 46.0 | 6.5 | 92.5 | 32.5 | 43.5 | 1.5 |
| 200M | Ours | 99.0 | 100.0 | 100 | 97.0 | 54.5 | 100.0 | 99.0 | 17.5 | 90.5 | 97.5 | 46.0 | 43.5 |
| | Gato | 51.0 | 58 | 84.5 | 56.5 | 35.5 | 53.5 | 49.0 | 15.0 | 65.0 | 52.0 | 33.0 | 0 |
| | Flamingo | 49.0 | 50.0 | 66.5 | 47.0 | 35 | 47.5 | 50.0 | 4.0 | 66.0 | 30.5 | 43.5 | 0.5 |
| | DT | 52.0 | 51.0 | 55.0 | 49.5 | 40.0 | 46 | 50.5 | 5.0 | 82.0 | 37.0 | 38.0 | 1.5 |

Table 12: L4 level generalization results. Model indicates robot controller parameter count.

| Model | Method | Task 08 | Task 10 | Task 13 | Task 14 |
|-------|----------|--------------|------------|----------|-------------|
| 2M | Ours | 6.5 | 0 | 0 | 96.5 |
| | Gato | 21.0 | 0.5 | 0 | 32 |
| | Flamingo | 22.0 | 0 | 0 | 27.5 |
| | DT | 22.5 | 0.0 | 0 | 22.0 |
| 20M | Ours | 100.0 | 0 | 0 | 95.5 |
| | Gato | 20.5 | 0.0 | 0 | 29 |
| | Flamingo | 21.0 | 0 | 0 | 27.5 |
| | DT | 20.5 | 0.5 | 0 | 36.0 |
| 200M | Ours | 100.0 | 0 | 0 | 94.5 |
| | Gato | 30.5 | 0.0 | 0 | 37 |
| | Flamingo | 24.5 | 0 | 0 | 24.0 |
| | DT | 20.0 | 0.0 | 0 | 28.5 |

F EXTENDED RELATED WORK

In this section, we provide an extended review of related work as complementary to Section 6.

Table 13: Performances of our method with different sized pre-trained T5 prompt encoder. We fix the parameter count of the decision-making part to be 200M.

| | t5-small (30M) | t5-base (111M) | t5-large (368M) |
|----|----------------|----------------|-----------------|
| L1 | 78.8 | 81.5 | 80.8 |
| L2 | 79.0 | 81.5 | 81.0 |
| L3 | 80.3 | 78.7 | 81.0 |
| L4 | 49.1 | 48.6 | 49.3 |

Multi-task Learning by Sequence Modeling. In NLP domain, the Natural Language Decathlon (McCann et al., 2018) adopts a consistent question-answering format for a suite of 10 NLP tasks. In computer vision, Mask R-CNN (He et al., 2017), UberNet (Kokkinos, 2016), and 12-in-1 (Lu et al., 2020) leverage a single backbone model with multiple independent heads for different tasks. UVim (Kolesnikov et al., 2022) is another unified approach for vision that uses a language model to generate the guiding code for a second model to predict raw vision outputs. In multimodal learning, numerous works (Lu et al., 2022; Wang et al., 2022a; Zellers et al., 2021; 2022; Buch et al., 2022; Fu et al., 2021; Yang et al., 2022) investigate the unification of image, video, audio, and/or language modalities to deliver multi-purpose foundation models, though most of which are not equipped with decision-making facilities. Perceivers (Jaegle et al., 2021b;a) propose an efficient architecture to handle general-purpose inputs and outputs. BEiT-3 (Wang et al., 2022c) performs masked data modeling on images, texts and image-text pairs to pre-train a backbone for various downstream tasks. MetaMorph (Gupta et al., 2022) learns a universal controller over a modular robot design space.

Foundation Models for Embodied Agents. Embodied agent research (Duan et al., 2022; Batra et al., 2020; Ravichandar et al., 2020; Collins et al., 2021) is adopting the large-scale pre-training paradigm, powered by a collection of learning environments (Abramson et al., 2020; Shridhar et al., 2020; Savva et al., 2019; Puig et al., 2018; Team et al., 2021; Toyama et al., 2021; Shi et al., 2017). From the aspect of **pre-training for better representations**, LaTTe (Bucker et al., 2022) and Embodied-CLIP (Khandelwal et al., 2021) leverage the frozen visual and textual representations of CLIP (Radford et al., 2021) for robotic manipulation.

Robot Manipulation and Benchmarks. There are many prior works that are not mentioned in the main paper that study different robotic manipulation tasks, such as constraint satisfaction (Bharadhwaj et al., 2021), one-shot imitation (Paine et al., 2018; Huang et al., 2019; Aceituno et al., 2021; Zhao et al., 2022), and rearrangement (Liu et al., 2021; Ehsani et al., 2021; Gan et al., 2021; Stengel-Eskin et al., 2022). Multiple simulation benchmarks are introduced to study the above tasks: 1) **Indoor simulation environments**: Habitat (Savva et al., 2019; Szot et al., 2021) is equipped with a high-performance 3D simulator for fast rendering and proposes a suite of common tasks for assistive robots. AI2-THOR (Ehsani et al., 2021; Deitke et al., 2022) is a framework that supports visual object manipulation and procedural generation of environments. 2) **Tabletop environments**: Meta-World (Yu et al., 2019), RL-Bench (James et al., 2019), and SURREAL (Fan et al., 2018; 2019) are widely used simulator benchmarks studying robotics manipulation with tabletop settings. Causal-World (Ahmed et al., 2021) is a benchmark for causal structure and transfer learning in manipulation, requiring long-horizon planning and precise low-level motor control. However, these simulators and benchmarks do not natively support task specification and prompting with multiple modalities.